Solomon

RADON-HAZARD POTENTIAL OF THE CENTRAL SEVIER VALLEY, SEVIER COUNTY, UTAH

Utah Geological Survey Special Study 89

RADON-HAZARD POTENTIAL OF THE CENTRAL SEVIER VALLEY, SEVIER COUNTY, UTAH

by
Barry J. Solomon

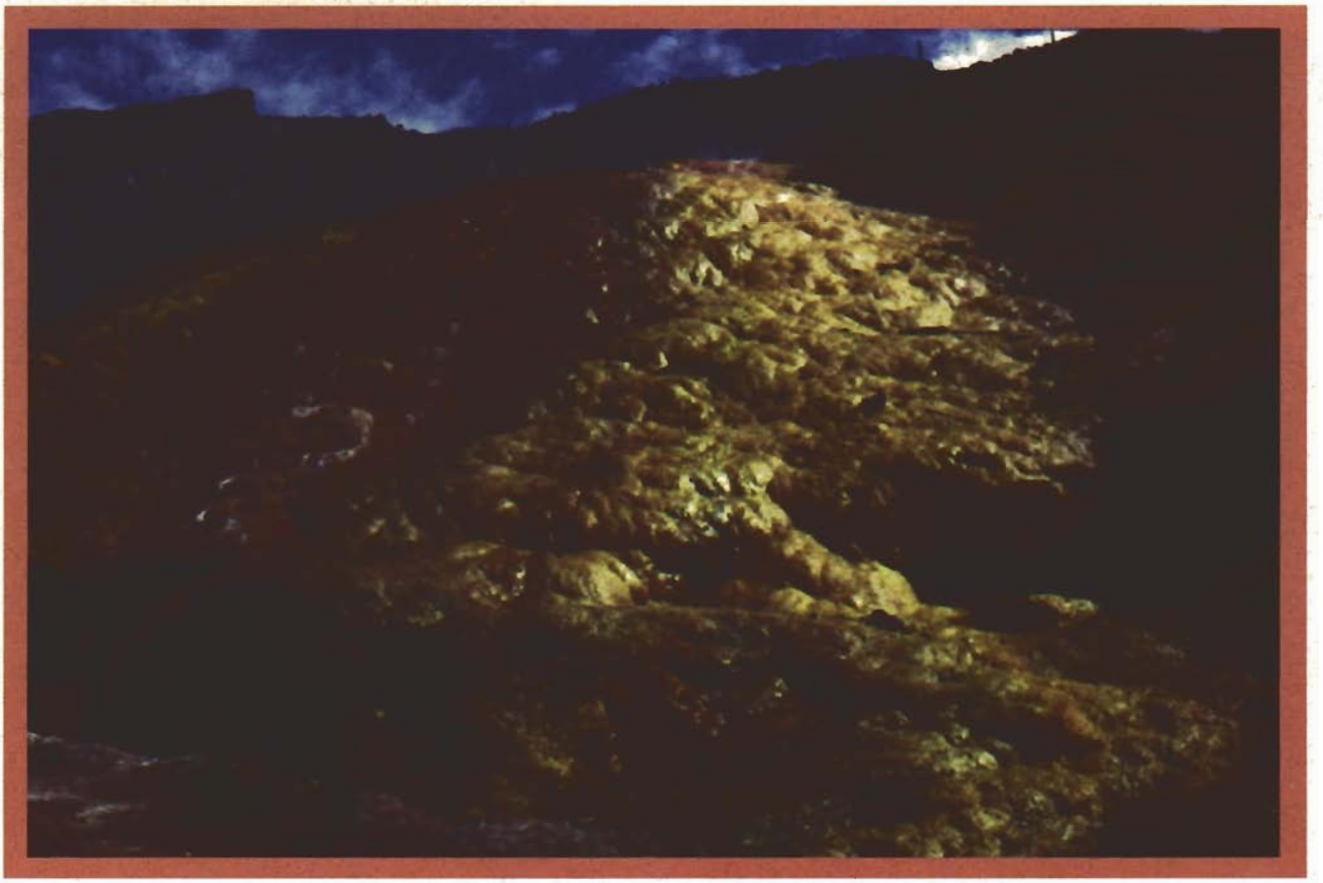

Travertine deposited by Red Hill Hot Springs along the Sevier fault zone near Monroe.

UTAH GEOLOGICAL SURVEY
SPECIAL STUDY 89

August 1996

UTAH DEPARTMENT OF NATURAL RESOURCES
in cooperation with
UTAH DEPARTMENT OF ENVIRONMENTAL QUALITY, DIVISION OF RADIATION CONTROL
and the
U.S. ENVIRONMENTAL PROTECTION AGENCY

RADON-HAZARD POTENTIAL OF THE CENTRAL SEVIER VALLEY, SEVIER COUNTY, UTAH

by
Barry J. Solomon

THIRD-YEAR GEOLOGIC STUDIES FOR THE U.S. ENVIRONMENTAL PROTECTION AGENCY STATE INDOOR RADON GRANT PROGRAM

SPECIAL STUDY 89
UTAH GEOLOGICAL SURVEY
a division of
UTAH DEPARTMENT OF NATURAL RESOURCES
in cooperation with
UTAH DEPARTMENT OF ENVIRONMENTAL QUALITY, DIVISION OF RADIATION CONTROL
and the
U.S. ENVIRONMENTAL PROTECTION AGENCY

ISBN 1-55791-374-9

Reference herein to any specific commercial product, process, or service by trade name, trademark, manufacturer, or otherwise, does not necessarily constitute or imply its endorsement, recommendation, or favoring by the Utah Geological Survey, the Utah Division of Radiation Control, or the U.S. Environmental Protection Agency. The views and opinions of the author expressed herein do not necessarily state or reflect those of the agencies.

STATE OF UTAH

Michael O. Leavitt, Governor

DEPARTMENT OF NATURAL RESOURCES

Ted Stewart, Executive Director

UTAH GEOLOGICAL SURVEY

M. Lee Allison, Director

UGS Board

Member	Representing
Russell C. Babcock, Jr. (chairman)	Mineral Industry
D. Cary Smith	Mineral Industry
Richard R. Kennedy	Civil Engineering
E.H. Deedee O'Brien	Public-at-Large
C. William Berge	Mineral Industry
Jerry Golden	Mineral Industry
Milton E. Wadsworth	Economics-Business/Scientific
David Terry, Director, Trust Lands Administration	*Ex officio member*

UGS Editorial Staff

J. Stringfellow	Editor
Vicky Clarke, Sharon Hamre	Graphic Artists
Patricia H. Speranza, James W. Parker, Lori Douglas	Cartographers

UTAH GEOLOGICAL SURVEY

The **UTAH GEOLOGICAL SURVEY** is organized into five geologic programs with Administration, Editorial, and Computer Resources providing necessary support to the programs. The **ECONOMIC GEOLOGY PROGRAM** undertakes studies to identify coal, geothermal, uranium, hydrocarbon, and industrial and metallic resources; initiates detailed studies of these resources including mining district and field studies; develops computerized resource data bases, to answer state, federal, and industry requests for information; and encourages the prudent development of Utah's geologic resources. The **APPLIED GEOLOGY PROGRAM** responds to requests from local and state governmental entities for engineering-geologic and ground-water investigations; and identifies, documents, and interprets Utah's geologic hazards and ground-water resources. The **GEOLOGIC MAPPING PROGRAM** maps the bedrock and surficial geology of the state at a regional scale by county and at a more detailed scale by quadrangle. The **GEOLOGIC EXTENSION SERVICE** answers inquiries from the public and provides information about Utah's geology in a non-technical format. The **PALEONTOLOGY AND PALEOECOLOGY PROGRAM** maintains and publishes records of Utah's fossil resources, provides paleontological recovery services to state and local governments, and conducts studies of environmental change to aid resource management.

The UGS Library is open to the public and contains many reference works on Utah geology and many unpublished documents on aspects of Utah geology by UGS staff and others. The UGS has several computer data bases with information on mineral and energy resources, geologic hazards, stratigraphic sections, and bibliographic references. Most files may be viewed by using the UGS Library. The UGS also manages a sample library which contains core, cuttings, and soil samples from mineral and petroleum drill holes and engineering geology investigations. Samples may be viewed at the Sample Library or requested as a loan for outside study.

The UGS publishes the results of its investigations in the form of maps, reports, and compilations of data that are accessible to the public. For information on UGS publications, contact the Sales Office, 2363 South Foothill Drive, Salt Lake City, Utah 84109-1491, (801) 467-0401.

The Utah Department of Natural Resources receives federal aid and prohibits discrimination on the basis of race, color, sex, age, national origin, or disability. For information or complaints regarding discrimination, contact Executive Director, Utah Department of Natural Resources, 1594 West North Temple #3710, Box 145610, Salt Lake City, UT 84116-5610 or Equal Employment Opportunity Commission, 1801 L Street, NW, Washington DC 20507.

Printed on recycled paper

3/96

CONTENTS

ABSTRACT . . . 1
INTRODUCTION . . . 2
SAMPLING METHODS . . . 4
DATA AND DISCUSSION . . . 5
Geology . . . 5
Uranium Concentrations . . . 10
Ground-Water Levels . . . 12
Soil Permeability . . . 14
Soil-Gas Radon . . . 17
Indoor Radon . . . 19
Other Radiometric Measurements . . . 22
RADON-HAZARD POTENTIAL . . . 26
Hazard Distribution . . . 29
Hazard Potential and Soil-Gas-Radon Levels . . . 32
Hazard Potential and Indoor-Radon Levels . . . 32
Cautions When Using This Report . . . 33
CONCLUSIONS . . . 33
ACKNOWLEDGMENTS . . . 34
REFERENCES . . . 35
APPENDIX - Survey Data . . . 38

FIGURES

Figure 1. Index map of Utah . . . 2
Figure 2. The Pahvant Range and an adjacent rural area . . . 3
Figure 3. Location map of the central Sevier Valley . . . 3
Figure 4. Generalized geologic map of the central Sevier Valley . . . 6
Figure 5. The Middle Jurassic Arapien Shale . . . 8
Figure 6. The Paleocene Flagstaff Formation . . . 8
Figure 7. The Eocene Green River Formation . . . 8
Figure 8. Tertiary volcanic rocks . . . 9
Figure 9. The Miocene Sevier River Formation . . . 9
Figure 10. Travertine at Red Hill Hot Springs . . . 10
Figure 11. Histogram of uranium concentrations . . . 11
Figure 12. Normal probability diagram of uranium concentrations . . . 12
Figure 13. Contour map of uranium concentrations . . . 13
Figure 14. Contour map of depth to ground water . . . 15
Figure 15. Soil permeability . . . 16
Figure 16. Histogram of soil-gas-radon concentrations . . . 17
Figure 17. Scatter plot and linear regression of uranium and soil-gas-radon data pairs . . . 17
Figure 18. Contour map of soil-gas-radon concentrations . . . 20
Figure 19. Exclusion isolines of soil-gas-radon concentrations . . . 21
Figure 20. Comparison of residential indoor-radon concentrations . . . 22
Figure 21. Map of indoor-radon concentrations . . . 23
Figure 22. Histogram of potassium concentrations . . . 25
Figure 23. Scatter plot of uranium and potassium data pairs . . . 25
Figure 24. Histogram of thorium concentrations . . . 26
Figure 25. Scatter plot of uranium and thorium data pairs . . . 26
Figure 26. Contour map of thorium concentrations . . . 27
Figure 27. Contour map of eU/eTh ratios . . . 28
Figure 28. Histogram of total gamma concentrations . . . 29
Figure 29. Scatter plot of total gamma and thorium data pairs . . . 29
Figure 30. Indoor-radon-hazard potential of the central Sevier Valley . . . 31
Figure 31. Indoor-radon-hazard potential of Sevier County . . . 32

TABLES

Table 1. Statistical summary of radiometric data . . . 11
Table 2. Correlation coefficient matrix . . . 18
Table 3. Residential indoor-radon concentrations . . . 22
Table 4. School indoor-radon concentrations . . . 24
Table 5. Radon-hazard-potential matrix . . . 30
Table 6. Radon-hazard-potential categories . . . 30
Table 7. Residential indoor-radon concentrations in radon-hazard-potential categories . . . 33
Table A-1. Radiometric data exclusive of indoor-radon measurements . . . 39
Table A-2. Residential indoor-radon measurements . . . 45
Table A-3. School indoor-radon measurements . . . 47

RADON-HAZARD POTENTIAL OF THE CENTRAL SEVIER VALLEY, SEVIER COUNTY, UTAH

by
Barry J. Solomon

ABSTRACT

Radon (^{222}Rn), a radioactive gas derived from the decay of uranium (^{238}U), occurs naturally in rock and soil. The gas migrates through the ground and, after penetrating foundation openings, can accumulate indoors in sufficient quantities to cause lung cancer. Both non-geologic and geologic factors influence indoor-radon concentrations. The effects of non-geologic factors, such as construction type and weather, are difficult to estimate. However, important geologic factors can be measured and their influence evaluated.

The geologic factors of uranium concentration, ground-water depth, and soil permeability are characterized for the central Sevier Valley in Sevier County, Utah, an area where indoor-radon concentrations up to 22.4 picocuries per liter (pCi/L) (829 Becquerels per cubic meter [Bq/m^3]) are found. Numerical scores were applied to each factor; higher scores correspond to conditions favorable for elevated indoor-radon concentrations. Three radon-hazard-potential categories were established based on cumulative totals of the three factors. The categories indicate the relative potential for elevated indoor-radon levels, and their areal distribution is delineated on a hazard map constructed from overlays for each factor.

The radon-hazard potential of the central Sevier Valley is highest in the south-central part of the valley between the city of Monroe and the community of Sevier, and northward along the valley margins. In these high-hazard areas, uranium-enriched geologic materials produce abundant radon gas that travels easily through coarse-grained, permeable alluvium. Radon migration through the well-drained soil is unimpeded by ground water which, if present, would dissolve the radon gas and render it unavailable for upward migration into buildings. The radon-hazard potential is lowest along the valley axis, north of the community of Central and the town of Annabella, where uranium-deficient soil is impermeable and poorly drained, soil-gas radon levels are low, and radon migration is hindered.

Uranium-enriched soil in the central Sevier Valley is derived from intermediate to silicic volcanic rocks of Tertiary age. Uranium-deficient soil is derived from shale and limestone of Jurassic and Tertiary age. Where radon-hazard potential is greatest, uranium concentrations exceed 3 parts per million (ppm) and reach a maximum of 14.1 ppm at Red Hill Hot Springs, northeast of Monroe. Levels of radon in soil gas are highest, up to 1,108 pCi/L (4.10×10^4 Bq/m^3), in areas with high uranium concentrations.

Linear regression of radon-uranium data pairs shows that concentrations in the central Sevier Valley are related by the formula $Rn = 29.2U + 136.1$, where Rn is the concentration of soil-gas radon in pCi/L and U is the concentration of uranium in ppm. Although statistically significant, the relationship is imperfect and has been affected by both disequilibrium between material at the ground surface tested for uranium and material at shallow depth tested for soil-gas radon, and the effects of soil permeability on the soil-gas sampling apparatus. Soil-gas radon levels analyzed with exclusion isolines, a semiquantitative technique which minimizes the effect of factors which differentially reduce concentrations, more closely correspond to uranium concentrations and hazard potential.

INTRODUCTION

Health officials believe that breathing elevated levels of radon gas over time increases an individual's risk of lung cancer (National Council on Radiation Protection and Measurements, 1984; Samet, 1989). In 1988, in response to growing national concern over the threat of radon gas, Congress enacted Title III, Indoor Radon Abatement Act (IRAA), as an amendment to the Toxic Substances Control Act. The goal of the IRAA is to reduce public-health risks from radon gas by rendering air within buildings in the United States free of radon. Section 306 of the IRAA authorizes the U.S. Environmental Protection Agency (EPA) to provide grants to states to support the development and implementation of state radon-assessment and mitigation programs. In 1989, the EPA established the State Indoor Radon Grants (SIRG) Program to implement Section 306 (U.S. Environmental Protection Agency, 1989a).

A principal SIRG activity of the Utah Geological Survey (UGS) is to assess the radon-hazard potential of the state and identify areas that have geologic factors conducive to elevated indoor-radon levels. Indoor-radon levels depend on both geologic and non-geologic factors. Four principal factors contribute to elevated indoor-radon concentrations: (1) elevated uranium levels in the soil or rock on which a structure is built, (2) soil and ground-water conditions that do not restrict the movement of radon, (3) porous building materials or foundation openings below grade, and (4) lower atmospheric pressure inside a building than outside (Tanner, 1986). Factors (1) and (2) are geologic factors that can be measured and characterized regionally; their effects vary locally but generally are predictable. Factors (3) and (4) are non-geologic factors that are difficult to measure and cannot be characterized regionally; their effects are variable and fluctuate with the weather, construction type, and occupant lifestyle. Thus, although the same radon-hazard potential from geologic factors may exist, indoor-radon levels can still vary from one structure to the next.

The EPA recommends reducing indoor radon when levels exceed 4 picocuries per liter (pCi/L) (148 Becquerels per cubic meter [Bq/m^3]) (U.S. Environmental Protection Agency, 1992). Levels of indoor radon greater than 4 pCi/L (148 Bq/m^3) were measured locally in the central Sevier Valley during a 1987-88 statewide survey conducted by the Utah Division of Radiation Control (UDRC) (Sprinkel and Solomon, 1990). However, the number of samples in the survey was insufficient to accurately delineate larger areas where elevated levels of radon are likely to occur. An evaluation of geologic factors conducive to elevated indoor-radon levels was therefore undertaken during the third year of the multi-year SIRG program to delineate the hazard in the central Sevier Valley. The hazard map can be used by decision makers to allocate funds toward public-information programs and testing in areas more likely to have elevated indoor-radon levels, and guide the use of radon-resistant new construction.

The central Sevier Valley trends northeastward for 38 miles (61 km) in western Sevier County, south-central Utah (figure 1). The valley is about 6 miles (10 km) wide. The Sevier River flows northeastward along the valley floor at elevations from 5,100 to 5,400 feet (1,550 to 1,650 m). The valley is bounded on the west by the Pahvant Range, which reaches elevations of more than 10,000 feet (3,000 m), and on the east by the Sevier Plateau, which reaches elevations of more than 11,000 feet (3,400 m). The valley is principally a rural area with a small population and low population density (figure 2). The largest cities in the valley are Richfield (population 5,593), Salina (population 1,943), Monroe (population 1,472), and Aurora (population 911) (Utah Office of Planning and Budget, 1991) (figure 3). Most residents are engaged in agriculture and related activities. The climate in the valley is semiarid, with an annual precipitation of less than 10 inches (25 cm) on the valley floor. From the first of November through March most precipitation is snow.

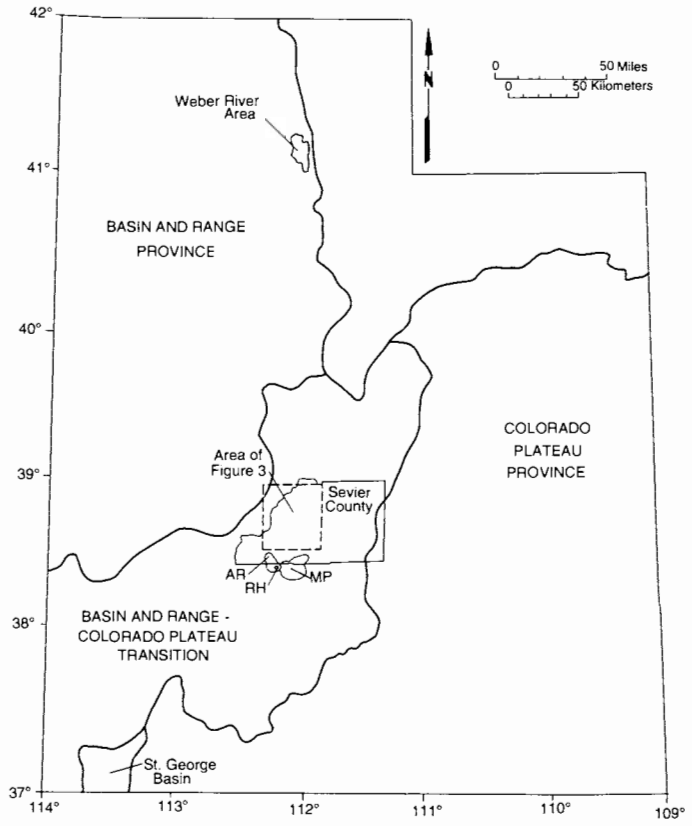

Figure 1. Index map of Utah showing physiographic subdivisions (modified from Stokes, 1977) and locations discussed in text. AR - Antelope Range, MP - Monroe Peak Caldera, RH - Red Hills Caldera.

Three geologic factors were evaluated to determine the radon-hazard potential in the central Sevier Valley: (1) uranium concentration in shallow soil, (2) ground-water depth, and (3) soil permeability. Uranium concentrations measured in this study were combined with ground-water depth and soil-permeability data from existing sources to derive maps showing relative indoor-radon-hazard potential. Uranium (^{238}U) concentration is a primary geologic prerequisite for elevated indoor-radon levels because the most abundant radon isotope, ^{222}Rn, forms by the decay of uranium. Meussig (1988) shows a correlation between areas with mean equivalent uranium (eU) concentrations greater than 2.4 parts per million (ppm) and indoor-radon levels greater than 4 pCi/L (148 Bq/m^3). However,

Figure 2. *The Pahvant Range, in the distance, and an adjacent, typically rural area of the central Sevier Valley southwest of Aurora, in the middle distance.*

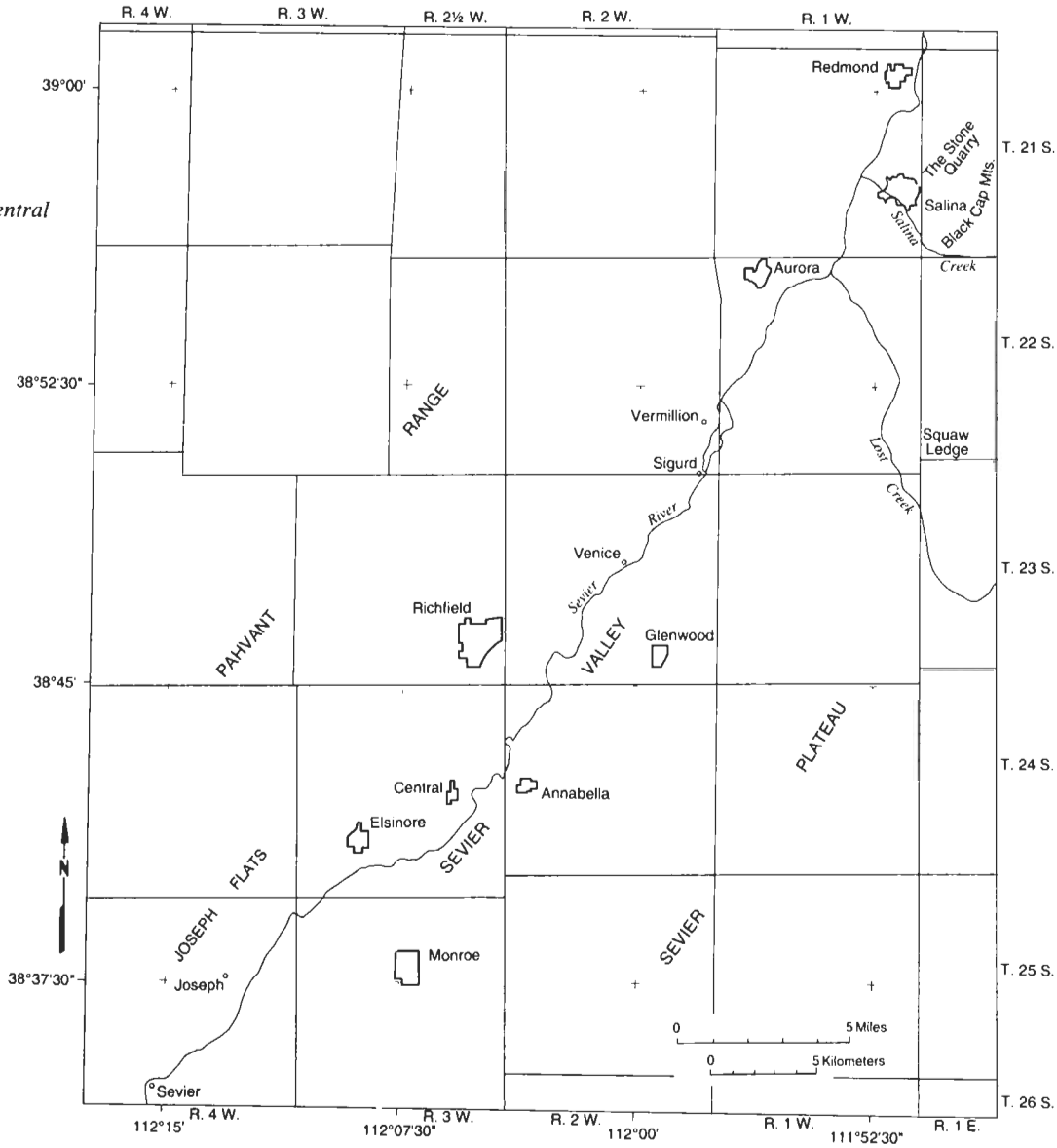

Figure 3. *Location map of the central Sevier Valley.*

even if radon is generated in sufficient quantity by uraniferous foundation soil, pore water in the soil effectively traps radon and inhibits radon migration (Tanner, 1980). Conversely, low soil-moisture content above the ground-water table facilitates diffusion of radon to the air. The rate of radon migration is a function of soil permeability. Permeable soil with open pathways enables radon migration, whereas impermeable soil inhibits radon migration, whether by diffusion of soil gas or ground-water transport (Schery and Siegel, 1986).

In addition to the three geologic factors used for hazard evaluation, concentrations of five other geochemical factors were measured: (1) thorium (^{232}Th) in shallow soil, (2) potassium (^{40}K) in shallow soil, (3) total gamma count in shallow soil, (4) radon in soil gas, and (5) indoor radon. Although ^{222}Rn is generally the most significant contributor to indoor radon, ^{220}Rn may also be significant if in sufficient quantities (Stranden, 1984). This latter radon isotope is formed by the decay of ^{232}Th. Variations in valley-fill material of U, Th, and K concentrations and total gamma count reflect characteristic geochemical signatures of certain bedrock lithologies and indicate potential source rocks in adjacent mountains (Nielson and others, 1991). Soil-gas radon levels reflect variations in uranium concentration, ground-water level, and soil permeability, and soil-gas levels can validate assessed relative hazard potential determined from primary geologic factors (Solomon and others, 1993). Additional indoor-radon levels were also measured for comparison with mapped hazard potential.

SAMPLING METHODS

Three techniques were used to collect radiometric data during geophysical surveys: (1) gamma-ray spectrometry measures concentrations of radioactive elements including uranium and thorium, the parent materials of radon in soil gas; (2) radon emanometry measures levels of soil-gas radon available for migration into buildings; and (3) alpha-track detectors (ATDs) measure indoor-radon levels. With the exception of indoor-radon measurements, the surveys were conducted from August 29 through October 22, 1992 by the UGS. Residential indoor-radon levels were first measured in the central Sevier Valley as part of a statewide sampling in 1987-88 (Sprinkel and Solomon, 1990), and additional measurements were collected in a targeted survey during 1992-93. Indoor-radon levels in selected schools were measured during the 1990-91 school year. All indoor-radon levels were measured by the UDRC.

Concentrations of gamma-emitting elements in soil were determined using an Exploranium GR-256 portable gamma-ray spectrometer, with a GPS-21 detector. The detector assembly contains a 3 x 3 inch (7.5 x 7.5 cm) sodium-iodide crystal with an integral bi-alkali photomultiplier tube. Values for total gamma, ^{40}K (K), equivalent ^{238}U (eU), and equivalent ^{232}Th (eTh) were collected. Peak energy levels measured were 1.46 million electron volts (MeV) for K (which has only one emission line), 1.76 MeV for eU (corresponding to Bismuth [^{214}Bi]), and 2.62 MeV for eTh (corresponding to Thalium [^{208}Tl]). The spectrometer was calibrated at the factory using calibration pads. Survey stations were spaced about 1.0 mile (1.6 km) apart; exact spacing depended upon access. Measurement on roadbeds was avoided to reduce the possibility of masking by foreign materials. The detector was held at a height of about 2 feet (0.6 m) to correct for the influence of local topography and non-homogenous materials. Spectrometer measurements were conducted at 202 sites.

Radon concentrations in soil were determined using an RDA-200 portable alpha-sensitive scintillometer manufactured by EDA Instruments. This apparatus employs an active method of soil-gas extraction using a hollow probe and hand-held pump rather than a passive method of radon detection using, for example, ATDs. Detection of radon by passive methods depends primarily on diffusion of radon from the ground toward the cavity in which the detector is located and, because radon decays *en route*, the true radon concentration is underestimated (Tanner, 1991a).

Soil gas is pumped into scintillator cells placed into the scintillometer for measurement of radon concentrations. Scintillator cells are coated with a phosphor sensitive to alpha particles in the 5.5 MeV range emitted by the decay of isotopic radon in its gas phase. The cells were calibrated in the Geotech, Inc. alpha-track chamber to determine the efficiency of the phosphor material coating the cells. The scintillometer was calibrated at the factory, and the unit's sensitivity was checked against a standard test cell with a known count rate to account for gradual changes in the sensitivity of the photomultiplier tube.

The soil-gas sampling system consisted of a 0.5-inch (1.3-cm) diameter, hollow steel probe that was placed into a hole made by pounding a solid steel rod of the same diameter into the soil. The probe was inserted to a depth of about 26 inches (65 cm), and samples were collected from perforations in the lower 6 inches (15 cm) of the probe. This depth enabled samples to be collected below the root zone for grasses, within the lower B or upper C soil horizons, and close to sampling depths which provided consistent and reproducible data to other researchers (Reimer and Bowles, 1979; Hesselbom, 1985; Reimer and Gundersen, 1989). A hand-held evacuation pump was used to purge the probe of ambient air and pump soil gas into the scintillator cells. Samples were collected from vacant lots and undeveloped, non-irrigated land. Soil-gas samples were collected from 99 of the 202 sites at which spectrometer readings were taken. Samples from the remainder of the sites were not collected either because probe refusal occurred in dense soil or shallow bedrock; dry, sandy soils collapsed before the probe could be inserted; or spectrometer readings were taken merely to fill data gaps and, therefore, soil-gas sample collection was not attempted. A delay time of 2 to 3 hours between sample collection and measurement was used to allow for decay of the short-lived ^{220}Rn isotope and radon daughters, and ensure measurement of only ^{222}Rn.

Indoor-radon levels were measured for a one-year period with ATDs placed in the lowest occupied living space of single-family, owner-occupied homes, as well as in basement school rooms or ground-floor rooms of schools without basements. ATDs manufactured by Terradex Corporation were used in 14 homes during the 1987-88 statewide survey, and ATDs manufactured by Alpha Spectra, Inc. were used in three schools during the 1990-91 school year and 24 homes during the 1992-93 targeted survey. School testing was conducted in accordance

with EPA guidance, which suggests normal school-room occupancy and normal operating procedures for central heating, ventilation, and air-conditioning systems during the measurement period (U.S. Environmental Protection Agency, 1989b). Duplicate detectors were used to analyze the precision of school measurements, and field blanks (control detectors) were used to determine the extent of exposure to extraneous radiation sources.

DATA AND DISCUSSION

The central Sevier Valley is located in the transition zone between the Colorado Plateau and Basin and Range physiographic provinces (Stokes, 1977) (figure 1). Distinctive geologic structure and lithologies of this zone (figure 4) affect the distribution of geologic factors influencing the indoor-radon hazard.

Geology

The oldest rocks exposed on the flanks of the central Sevier Valley are fine-grained, gypsiferous beds of the Middle Jurassic Arapien Shale (Willis, 1986) (figure 5). This unit is intensely folded, faulted, and structurally thickened, and occupies the core of the Sanpete-Sevier Valley anticline (Gilliland, 1963) in the northeastern part of the study area (figure 4). Sediment derived from these rocks, between Glenwood and Salina on the northeastern margin of the central Sevier Valley, have low uranium and thorium concentrations and are relatively impermeable.

The Paleocene Flagstaff Formation, predominantly limestone, is present in the Pahvant Range on the west-central margin of the study area (Lautenschlager, 1952; Willis, 1994) (figures 4 and 6). These rocks dip gently eastward beneath the valley. An early interpretation suggested that the rocks were bounded by a major range-front fault identified as the Elsinore Fault by Callaghan and Parker (1961), but the structure is now assumed to be part of a southeast-facing monocline (Anderson and Barnhard, 1992). Sediment derived from these rocks, between Richfield and Vermillion on the northwestern margin of the central Sevier Valley, also have low uranium and thorium concentrations and are relatively impermeable.

The Flagstaff Formation is overlain to the northeast and south by the Eocene Green River Formation and several other sedimentary units of Eocene and Oligocene age (Willis, 1988) (figure 7). Like the older Arapien and Flagstaff units, the Eocene and Oligocene rocks are predominantly shale and limestone. Derived sediment also has low uranium and thorium concentrations and is relatively impermeable. The rocks are common on the northwestern margin of the central Sevier Valley; the Green River Formation is prevalent to the northwest in the Pahvant Range between Vermillion and Aurora, and other units of more limited extent crop out north of Aurora and southwest of Richfield.

Younger bedrock units surrounding the valley elsewhere, however, are distinctly different from these older sedimentary rocks. Volcanic rocks of intermediate composition, both flows and tuffs, were extruded to the surface beginning in the Oligocene and extending into the Miocene (Cunningham and others, 1983). This was followed in the Miocene by eruption of a bimodal suite of volcanic rocks of both basaltic and rhyolitic composition. The volcanic rocks, and associated intrusives, are related to numerous calderas in the region. The largest of these, the Monroe Peak Caldera, is adjacent to the southeastern corner of the study area (Rowley, Cunningham, and Kaplan, 1981) (figure 1). Another, the Red Hills Caldera, is 4 miles (6 km) south of the study area in the Antelope Range, and was the host of uranium veins in the prolific Central Mining Area (Cunningham and Steven, 1979) (figure 1). Many other volcanic and intrusive rocks in the vicinity of the central Sevier Valley are enriched in uranium and thorium, but at subeconomic levels.

The volcanic rocks are subdivided into a variety of units too extensive to list here, but some of the more voluminous units include the Bullion Canyon Volcanics of Miocene and Pliocene age on the southern valley margin between Monroe and Sevier (Rowley and others, 1988; Steven and Cunningham, 1979); the Miocene or Oligocene Tuff of Albinus Canyon on the southwestern valley margin between Elsinore and Richfield (Steven, 1979); and the Miocene Osiris Tuff south of Monroe (Rowley, Cunningham, and Kaplan, 1981) and east of Salina (Willis, 1986) (figure 8). The volcanic units are widespread in the mountains surrounding the southern half of the study area and extend along the eastern margin of the valley northward to the vicinity of Redmond, where associated volcaniclastic sedimentary deposits are also found (Willis, 1991) (figure 4).

The Miocene Sevier River Formation overlies older bedrock units in scattered areas around the valley margin (Steven and others, 1990) and, with unconsolidated Quaternary sediments within the valley, are locally derived deposits that reflect the uranium and thorium concentrations of adjacent, older bedrock. The Sevier River Formation consists of poorly to moderately consolidated clastic and carbonate rocks of fluvial and lacustrine origin (figure 9). Unconsolidated Quaternary sediments are predominantly mixtures of poorly sorted silt, sand, and gravel. The Quaternary sediments are commonly well drained, coarser grained, and most permeable along valley margins in alluvial-fan deposits on piedmont slopes, and are poorly drained, finer grained, and least permeable in alluvial floodplain deposits associated with the Sevier River.

Quaternary deposits of restricted extent but local importance to the radon hazard include hot-spring and landslide deposits. Deposits derived from hot springs are found along the Sevier and Dry Wash fault zones, which bound both margins of the valley in the southern part of the study area (figures 4 and 10). Anomalously high radon concentrations have been measured in Utah where there is active hydrothermal upwelling along faults (Nielson, 1978). Circulating fluid within the faults leaches uranium at depth and precipitates it in surficial hot-spring deposits. Monroe and Red Hill Hot Springs issue along the Sevier fault zone near Monroe, and Joseph Hot Springs issues along the Dry Wash fault zone near Joseph (Mabey and Budding, 1987) (figure 4). The fault zones themselves may contribute to elevated indoor-radon levels by increasing permeability and thereby enhancing near-surface radon concentrations (Tanner, 1980). Landslide deposits are found east of Monroe, where uraniferous volcanic debris in the Thompson Creek landslide generates significant

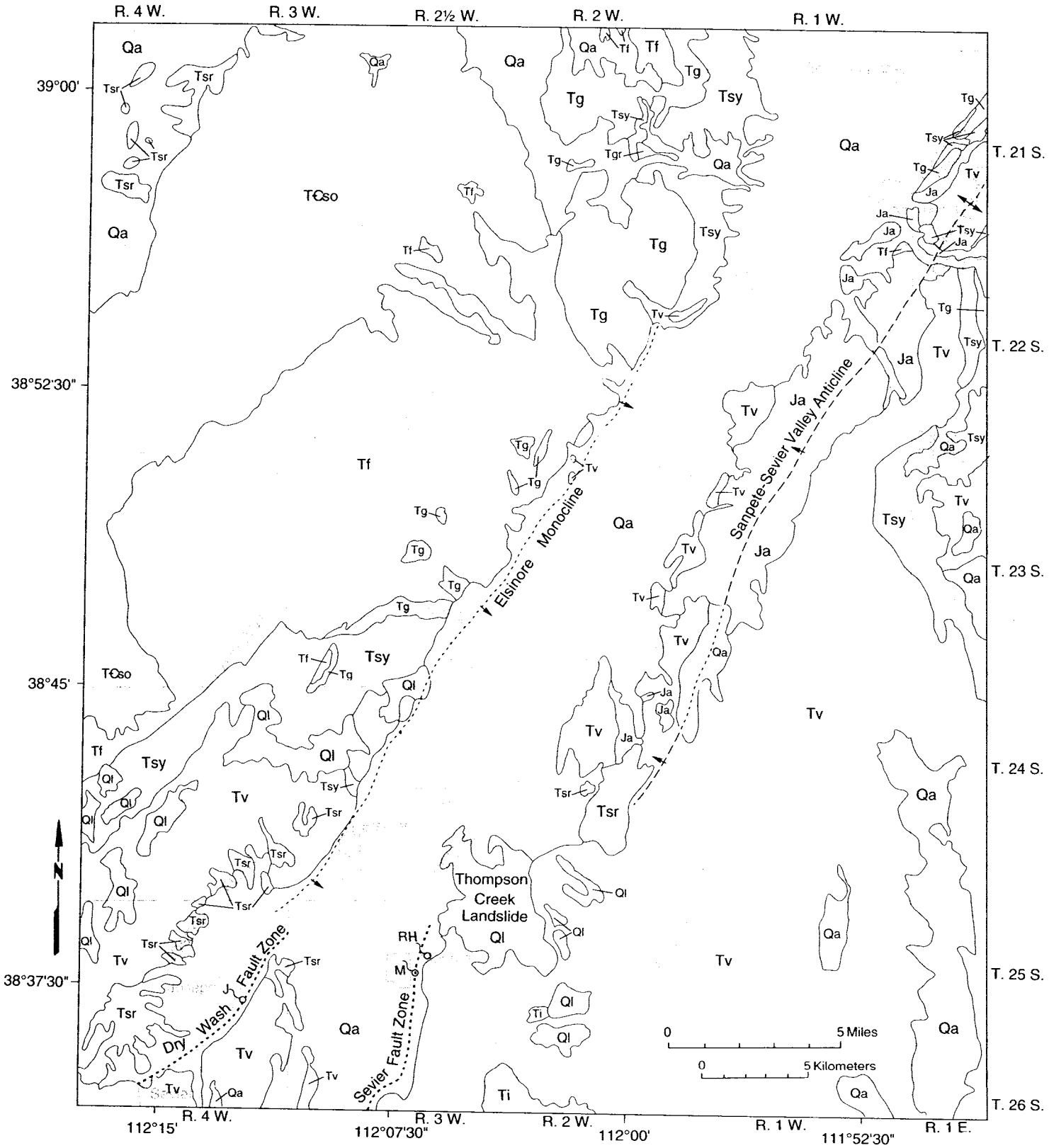

Figure 4. Generalized geologic map of the central Sevier Valley. Compiled and modified from Williams and Hackman (1971), Morris (1987), Witkind and others (1987), and Steven and others (1990).

***Figure 4** (continued)*

CORRELATION OF MAP UNITS

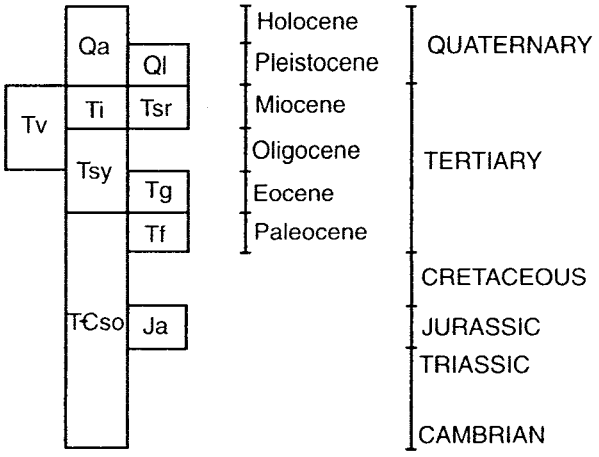

SYMBOLS

CONTACT

FAULT - Dotted where concealed

AXIS OF ANTICLINE - Dashed where approximate

AXIS OF MONOCLINE - Dashed where approximate, dotted where concealed

THERMAL SPRING - J - Joseph Hot Spring; M - Monroe Hot Spring; RH - Red Hill Hot Spring

DESCRIPTION OF MAP UNITS

Qa	Basin-fill deposits (Quaternary)
Ql	Landslide debris (Quaternary)
Tsr	Sevier River Formation (Miocene)
Ti	Plutons (Miocene)
Tv	Volcanic rocks (Miocene and Oligocene)
Tsy	Younger sedimentary rocks (Oligocene and Eocene)
Tg	Green River Formation (Eocene)
Tf	Flagstaff Formation (Paleocene)
T€so	Older sedimentary rocks (Paleocene to Cambrian)
Ja	Arapien Shale (Jurassic)

Figure 5. *Incised and deformed beds of the Middle Jurassic Arapien Shale, 4 miles (6 km) south of Salina on the south side of Lost Creek. Sediment derived from these fine-grained, gypsiferous rocks has low uranium and thorium concentrations and is relatively impermeable. Photo by G.C. Willis.*

Figure 6. *Gently dipping beds of the Paleocene Flagstaff Formation, 3 miles (5 km) north of Richfield in the foothills of the Pahvant Range. Sediment derived from these carbonate rocks also has low uranium and thorium concentrations and is relatively impermeable. Photo by G.C. Willis.*

Figure 7. *Hogback composed of the Eocene Green River Formation, 2 miles (3 km) northeast of Salina at The Stone Quarry. Like the older Arapien and Flagstaff units, rocks of the Green River Formation are predominantly shale and limestone, and derived sediment has low uranium and thorium concentrations and is relatively impermeable. Photo by G.C. Willis.*

Figure 8. *Outcrop of Tertiary volcanic rocks at Squaw Ledge, 6 miles (10 km) south of Salina. The ridge is capped by the Miocene Osiris Tuff, which is underlain by the Miocene or Oligocene Tuff of Albinus Canyon. These and similar volcanic units are typically enriched in uranium and thorium. Photo by G.C. Willis.*

Figure 9. *A gently sloping pediment overlies light-colored rocks of the Miocene Sevier River Formation near the southwest end of Joseph Flats. These locally derived deposits of poorly to moderately consolidated clastic and carbonate rocks are of fluvial and lacustrine origin and reflect the uranium and thorium concentrations of adjacent, older bedrock.*

Figure 10. Travertine deposited by Red Hill Hot Springs along the Sevier fault zone near Monroe. Elevated uranium and thorium concentrations were measured at the hot springs, and the fault zones may also contribute to elevated indoor-radon levels by increasing permeability and thereby enhancing near-surface radon concentrations.

levels of radon gas that easily migrate through permeable material.

The depositional and diagenetic history of these geologic units controls the characteristics of geologic factors relevant to the potential for elevated indoor-radon levels. However, factor characteristics are not uniform within each unit. Factor distribution is more accurately represented on overlays constructed irrespective of geologic contacts. Three factors are mapped on overlays: surficial-uranium concentration, ground-water level, and soil permeability. The distribution of two other measurements, soil-gas and indoor-radon concentration, are also mapped for comparison with geologic factors. Other radiometric data, including total gamma count and concentrations of K and eTh, are not mapped but are statistically summarized and their significance discussed. Data for each sample location are listed in appendix tables A-1, A-2, and A-3.

Uranium Concentrations

The airborne radiometric survey completed under the National Uranium Resource Evaluation (NURE) program provides a data base for the regional delineation of areas of high surface uranium concentrations, and can be used as an indicator of areas that have the potential for indoor-radon hazards (Duval, 1991). The NURE survey identified two major aerial radiometric anomalies in the central Sevier Valley: (1) in Tertiary volcanic rocks and adjacent Quaternary alluvium between Glenwood and Vermillion, in the east-central part of the study area; and (2) in similar rocks in the mountains south of Monroe and Sevier, along the southern edge of the study area (Bromfield and others, 1982; Lupe and others, 1982). NURE data in the central Sevier Valley, however, were collected on a coarse scale, generally with 5-kilometer (3-mi) line spacing and 20-kilometer (12-mi) spacing on tie lines, and tend to smooth out anomalies. A more detailed surface evaluation accurately delineates these regional anomalies and indicates other, local areas of higher concentrations.

Uranium concentrations in Quaternary basin fill were measured in the central Sevier Valley during a ground survey conducted for this study (figure 11). The mean concentration of uranium in the central Sevier Valley is 3.6 ppm, with a standard deviation of 1.9. Distribution of uranium concentration is approximately lognormal, with a moderate positive skewness of 14.2 (table 1). A lognormal distribution, with many samples of relatively low concentration but a few of high concentration, is expected when trace elements are randomly distributed in a homogenous material (Rogers, 1964). However, considerable variation is associated with local stratigraphy.

Populations of data points, related to geologic units and sediment-source areas, are shown on the probability diagram of uranium concentrations (McCammon, 1980) (figure 12). Changes in the slope of the data correspond with thresholds that partition the curve into distinct data sets and coincide with amounts of the populations present (Sinclair, 1976). The uranium concentrations of the end-member populations are close to those of the ideal components from which the mixture is derived. A threshold at about 2 ppm (point 1 on figure 12) indicates that about 15 percent of the samples consist of Quaternary alluvium derived predominantly from adjacent outcrops of pre-volcanic sedimentary rocks with low uranium concentrations. Another threshold at about 6 ppm (point 2 on figure 12) indicates that about 5 percent of the samples consist of similar alluvium derived predominantly from adjacent outcrops of Tertiary volcanic rocks with high uranium concentrations. The remaining 80 percent of the samples are derived from varying mixtures of these two components, with their proportion a function of rock composition in the source area and the mode of sediment transport between areas of source and deposition. Material in alluvial-fan deposits, shed from adjacent range fronts, reflects the composition of nearby bedrock; material in floodplain deposits,

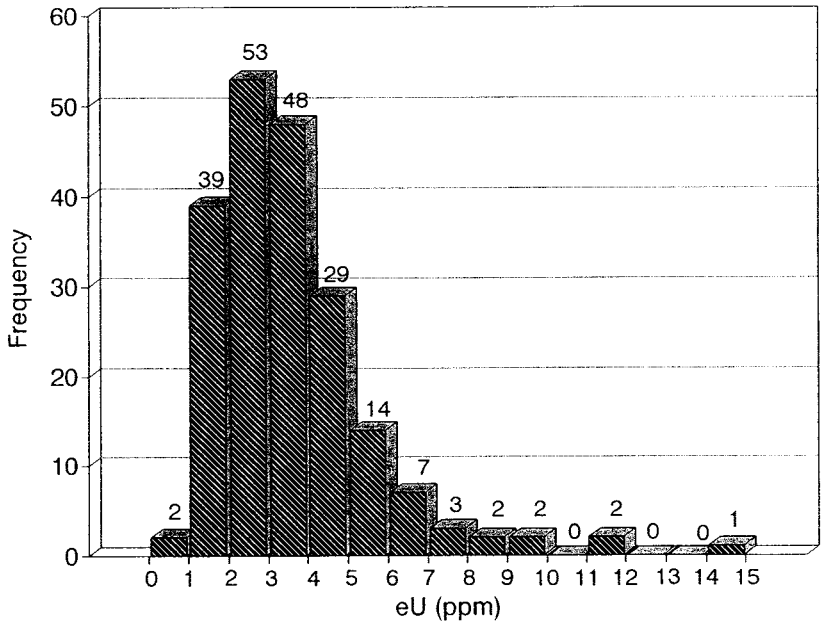

Figure 11. *Histogram of uranium (eU) concentrations from gamma-ray spectrometry in the central Sevier Valley. Distribution is approximately lognormal, with a moderate positive skewness. Lognormal distribution is expected when trace elements are randomly distributed in a homogenous material (Rogers, 1964).*

Table 1.

Statistical summary of radiometric data from the central Sevier Valley. Indoor-radon measurements are residential only, and do not include school data. K - potassium-40, eU - equivalent uranium-238, eTh - equivalent thorium-232, eU/eTh - ratio of eU and eTh, Rn - radon-222.

Statistic	Total Gamma (ppm)	K (%)	eU (ppm)	eTh (ppm)	eU/eTh	Soil-Gas Rn (pCi/L)	Indoor Rn (pCi/L)
Sample Size	202	202	202	202	202	99	38
Mean	14.3	1.9	3.6	11.1	0.37	240	4.9
Variance	54.3	0.9	3.6	48.2	0.02	37,837	23.9
Standard Deviation	7.4	0.9	1.9	6.9	0.16	195	4.9
Skewness	470.0	0.4	14.2	482.8	0.01	12,843,605	262.3
Minimum	4.1	0.3	0.9	2.4	0.13	0	0.3
25th %	9.0	1.2	2.3	6.0	0.27	106	1.7
Median	12.1	1.8	3.2	8.8	0.34	174	3.4
75th %	18.0	2.4	4.3	14.7	0.43	310	6.5
Maximum	43.5	4.4	14.1	41.9	1.18	1,108	22.4

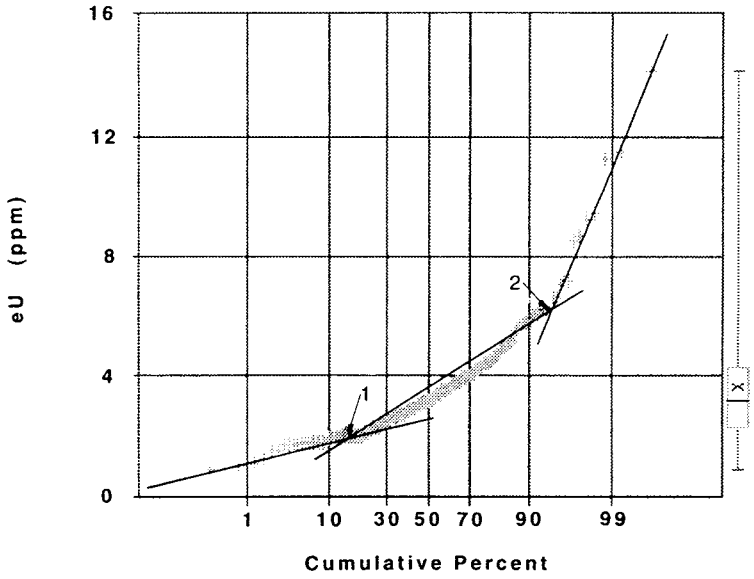

Figure 12. Normal probability diagram of uranium (eU) concentrations in the central Sevier Valley. Thresholds 1 and 2 are discussed in the text. The boxplot to the right of the diagram depicts the limits (the ends of the line which extends outward from the rectangle), quartiles (the ends of the rectangle), median (the solid line within the rectangle), and arithmetic mean (the "X" within the rectangle) of the data set.

transported along the valley axis, reflects a more diverse mixture of source material.

The most extensive area of uranium concentrations less than 2 ppm, including the lowest measured concentration of 0.9 ppm west of Sigurd, is in the central portion of the study area between Richfield and Vermillion (figure 13). This broad band of low uranium concentrations is underlain by poorly sorted mixtures of sand, silt, clay, gravel, and boulders in alluvial-fan deposits derived from pre-volcanic sedimentary rocks in adjacent mountains. Most such rocks are mapped within either the Middle Jurassic Arapien Shale, Paleocene Flagstaff Formation, or Eocene Green River Formation (figure 4).

Moderate uranium concentrations from 2.0 to 3.0 ppm are scattered throughout the valley, but are particularly common in the northern part of the study area west of Salina and in the central part of the study area near lower concentrations (figure 13). In the northern part of the study area, alluvial-fan deposits are derived from adjoining outcrops of the Miocene and Pliocene Sevier River Formation. The Sevier River Formation is locally tuffaceous, and conglomerates within the unit locally contain volcanic clasts. The limited amount of volcanic material is a likely source of moderate uranium concentrations in adjacent basin fill. In the central part of the study area, the alluvial deposits are transitional between similar material derived from pre-volcanic sedimentary rocks low in uranium and volcanic rocks high in uranium.

Uranium concentrations greater than 3 ppm are common in a large part of the southern study area, south of Richfield, and in smaller locales on northern valley margins near Glenwood, Salina, and Vermillion (figure 13). Most alluvium in these areas is derived from uraniferous Tertiary volcanic rock that is commonly composed of rhyolitic tuff. Elevated uranium levels in the tuff are consistent with concentration of the element in late-stage differentiation of igneous melts (Nielson and others, 1991). Uranium enrichment in the southern part of the study area coincides with the southernmost aerial radiometric anomaly identified in the NURE survey. Concentrations measured in the present study are commonly from 5 to 9 ppm, with a maximum of 14.1 ppm. Elevated uranium concentrations near Glenwood and Vermillion coincide with the northernmost aerial radiometric anomaly identified in the NURE survey. Concentrations measured in the present study are commonly from 3 to 9 ppm, with a maximum of 11.5 ppm. Elevated uranium concentrations near Salina are not associated with either aerial radiometric anomaly. Concentrations measured in the present study are similar in magnitude to those found near Glenwood and Vermillion, with a maximum of 11.3 ppm.

Uranium concentrations greater than the uppermost threshold (6 ppm) on the probability curve (figure 12) were measured in sediments derived from volcanic units and deposited in varied environments. Quaternary alluvial-fan deposits between Sevier and Monroe, with uranium concentrations up to 8.6 ppm, were derived from nearby outcrops of the Joe Lott Tuff Member of the Miocene Mount Belknap Volcanics, a potential source of uranium transported in leachate to the vein deposits of the region (Carmony, 1977). Quaternary travertine near Monroe, where the highest uranium level in this study (14.1 ppm) was recorded in the southernmost NURE aerial radiometric anomaly, is associated with Red Hill Hot Springs, a permeable conduit for the circulation of uranium-enriched ground water. Quaternary landslide deposits east of Monroe in the Thompson Creek landslide, where a uranium concentration of 7.1 ppm was measured, are composed of permeable debris from the Miocene and Oligocene volcanic rocks of Koosharem (Rowley, Steven, and Kaplan, 1981). Quaternary alluvium near Glenwood and Vermillion is derived from nearby outcrops of Oligocene and Miocene (?) volcanic flows (Williams and Hackman, 1971), where the highest uranium level in the northernmost NURE aerial radiometric anomaly (11.5 ppm) was measured east of Glenwood. The highest concentration of uranium east of Salina (11.3 ppm) was measured on an outcrop of the Miocene Osiris Tuff on the west edge of Black Cap Mountain. The Osiris Tuff, where present near Monroe, was postulated as an alternate source of uranium in nearby vein deposits (Bromfield and others, 1982).

Ground-Water Levels

Pore water effectively traps radon and, if pores are saturated, inhibits radon migration in soil (Tanner, 1980). Conversely, low moisture content above the ground-water table facilitates diffusion of radon to the air and to buildings. An evaluation of ground-water levels, particularly where uranium concentrations are elevated, is useful to determine areas in which shallow ground water inhibits radon migration.

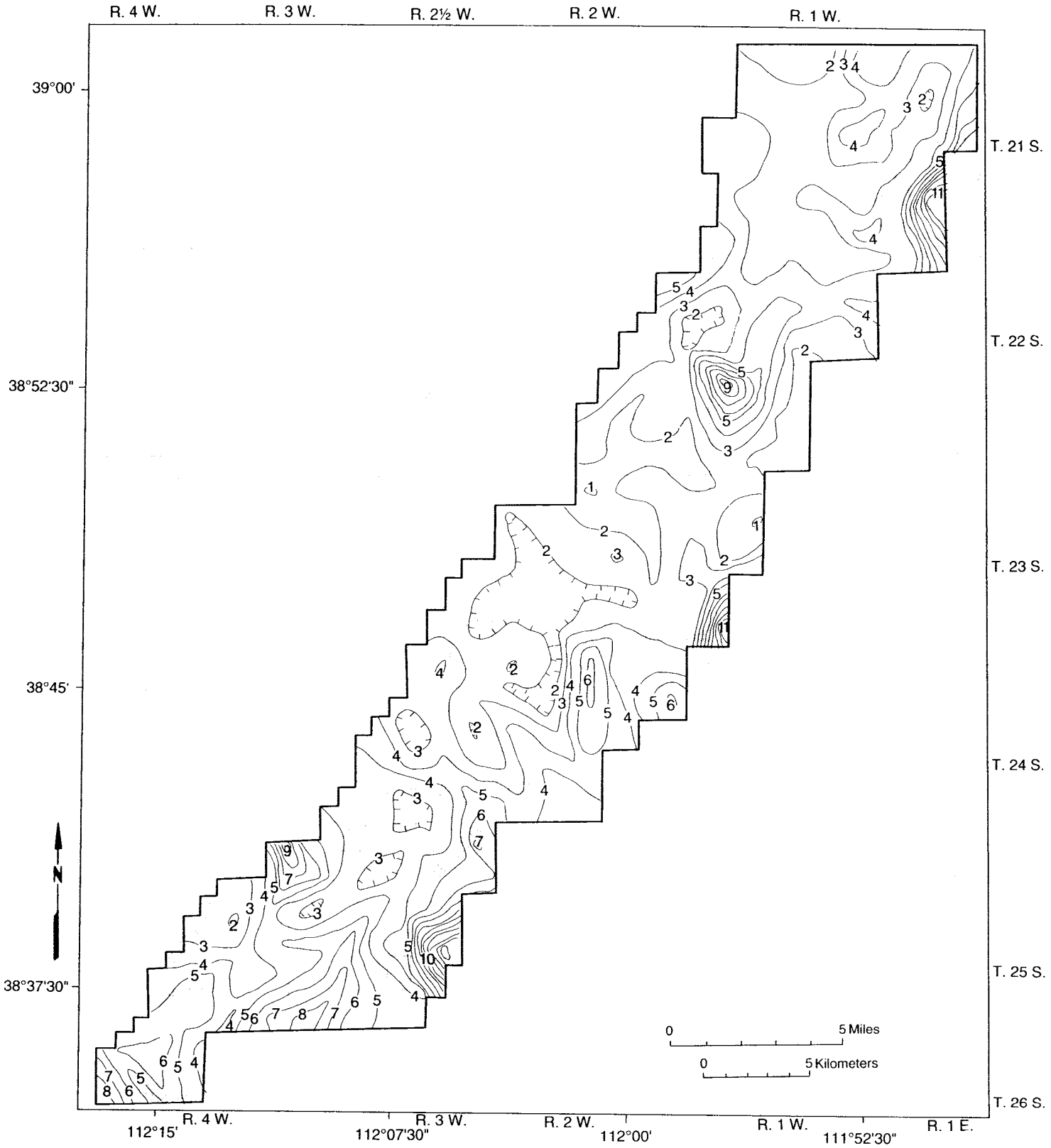

Figure 13. *Uranium (eU) concentrations from gamma-ray spectrometry in the central Sevier Valley. Contour interval is 1 ppm. Uranium concentrations greater than 3 ppm are common in Quaternary alluvium derived from uraniferous Tertiary rhyolitic tuff. Base map from U.S. Geological Survey Delta (1972), Price (1970), Richfield (1972), and Salina (1970) 1 x 2 degree topographic quadrangle maps. Contour interval is 200 feet (60 m).*

Most ground water in the central Sevier Valley is in coarse alluvial sand and gravel deposits beneath the valley floor (Young and Carpenter, 1965). Ground water exists under both artesian (confined) and water-table (unconfined) conditions. Where artesian conditions prevail near Richfield, the uppermost confining layer in the alluvium is 60 to 80 feet (18 to 24 m) thick. Where water-table conditions prevail, depth to water ranges from the land surface along the Sevier River to 180 feet (55 m) on valley margins.

Figure 14 shows the depth to ground water in unconsolidated deposits of the central Sevier Valley. Areas of shallow ground water, where it is discharged through springs and by evapotranspiration, are delineated by the distribution of phreatophytes and flowing wells (Young and Carpenter, 1965). Phreatophytes are plants that depend for their water supply on ground water that lies within reach of their roots (Robinson, 1958). Flowing wells are found in areas of phreatophyte growth and indicate that upward leakage through confining layers may help recharge the shallow aquifer. Flat valley floors, springs, marshes, oxbow lakes, and shallow wells are found in zones defined by phreatophytes and flowing wells and thus indicate that corresponding water depths are probably 10 feet (3 m) or less (Hecker and others, 1988).

Consolidated bedrock locally contains some ground water, but the rocks are generally ground-water barriers. The distribution of shallow ground water in the central Sevier Valley (figure 14) indicates the presence of two distinct ground-water basins separated by a bedrock constriction where the valley narrows (Young and Carpenter, 1965). The Aurora-Redmond basin to the north is separated from the Sevier-Sigurd basin by a bedrock constriction near the town of Vermillion. This pattern is repeated both to the north and south of the study area. The Aurora-Redmond basin is separated from the Redmond-Gunnison basin to the north by a constriction near the town of Redmond, and the Sevier-Sigurd basin is separated from the Junction-Marysvale basin to the south by a constriction south of the town of Sevier. In each case, the shallow, unconfined aquifer is recharged in the upper portions of the basins, and ground water is shallow and discharges where forced upward by bedrock constrictions in the lower portions of the basins.

Water levels greater than 50 feet (15 m) deep, along valley margins and just downstream from bedrock constrictions between ground-water basins, do not affect shallow radon migration. Water levels in unconsolidated, unconfined aquifers along the Sevier River, however, are commonly less than 50 feet (15 m) deep (figure 14) and, in the central portions of the ground-water basins, generally less than 10 feet (3 m) deep and sometimes near the land surface (Carpenter and Young, 1963). Ground water at depths less than 10 feet (3 m) is within the construction zone for basements. Should soil with high levels of uranium contact basement walls, shallow ground water may reduce otherwise potentially high radon levels. In other areas of the central Sevier Valley underlain by unconfined aquifers, water levels are between depths of 10 and 50 feet (3 and 15 m). Although a significant portion of radon generated from soil at these depths will have already decayed (the half-life of radon is 3.825 days) during upward migration prior to reaching basements, ground water in these areas also inhibits radon migration when seasonal variations cause ground-water levels to rise. Local perched ground-water conditions may be present anywhere in the study area, but consideration of their effects, as well as those of seasonal ground-water level variations, is beyond the scope of this study.

Soil Permeability

Once radon gas forms, it may migrate through the soil into buildings. A measure of the ability of radon to migrate through porous soil is permeability. The U.S. Soil Conservation Service (SCS) mapped soils in the central Sevier Valley (Wilson and others, 1958), and assigned permeability classes based on soil texture. Soils in the study area fall within six SCS permeability classes characterized by hydraulic conductivities which range from less than 0.06 to 20.0 inches/hour (4.2×10^{-5} to 1.4×10^{-2} cm/sec).

The six SCS permeability classes were combined for this study into three groups, based on the hydraulic conductivity of the thickest interval in the upper 5 feet (1.5 m) of soil. Well-drained soils, with hydraulic conductivities ranging from 6.0 to 20.0 inches/hour (4.2×10^{-3} to 1.4×10^{-2} cm/sec), are highly permeable and provide excellent pathways for radon migration (McLemore and others, 1991). Clay-rich soils, with hydraulic conductivities less than 0.6 inches/hour (4.2×10^{-4} cm/sec), are normally least permeable but may become more permeable if desiccation cracks form (Peake and Schumann, 1991). Soils with intermediate hydraulic conductivities ranging from 0.6 to 6.0 inches/hour (4.2×10^{-4} to 4.2×10^{-3} cm/sec) are moderately permeable.

The SCS classification is based upon the permeability of soil to the flow of water. The permeability of soil to the flow of gas is almost identical, with one significant exception -- sandy clay is more permeable to soil gas than to water (Rogers and Nielson, 1990). Sandy clay was therefore designated in this study as a moderately permeable soil, whereas the SCS classification designated sandy clay as least permeable.

Areas underlain by permeable rock, with or without a thin cover of residual soil, also affect radon-migration potential. However, one study (Schery and others, 1982) has shown that the presence of large fractures in bedrock does not significantly increase radon flux due to diffusion. The authors speculate that the volume of studied fractures may not have been significant enough to influence the bulk porosity and diffusion coefficients of exposed rock. In the central Sevier Valley, the permeability of small areas with exposed rock on valley margins is assumed to be the same as the permeability of adjacent unconsolidated material.

Permeability is highest in three small areas of the central Sevier Valley: (1) fluvial deposits of the Sevier River east of Joseph in the south end of the study area, (2) similar deposits of Salina Creek near Salina in the north end of the study area, and (3) alluvial-fan deposits at the mouths of small canyons from the Pahvant Range on the west-central margin of the study area (figure 15). Fluvial deposits consist of boulders, cobbles, gravel, sand, silt, and clay in mixtures that are moderately well sorted in

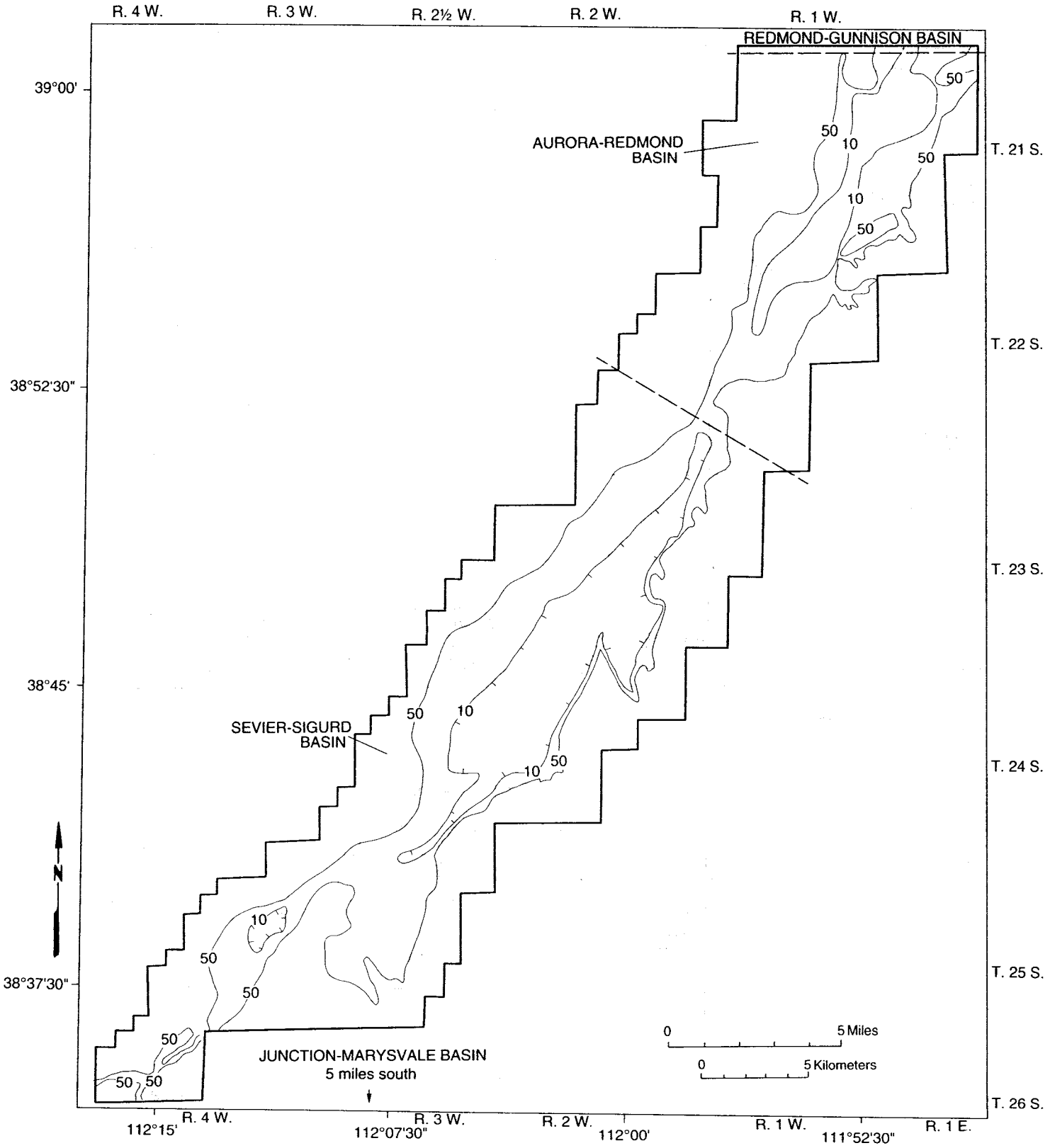

Figure 14. *Depth to ground water in unconsolidated material of the central Sevier Valley. Ground-water depth is defined by well data (Carpenter and Young, 1963; Young and Carpenter, 1965) and, where less than 10 feet (3 m) deep, by phreatophytes and flowing wells (Young and Carpenter, 1965, plate 5). Contours at depths of 10 and 50 feet (3 and 15 m). Boundaries between ground-water basins shown by dashed lines (from Young and Carpenter, 1965, plate 2).*

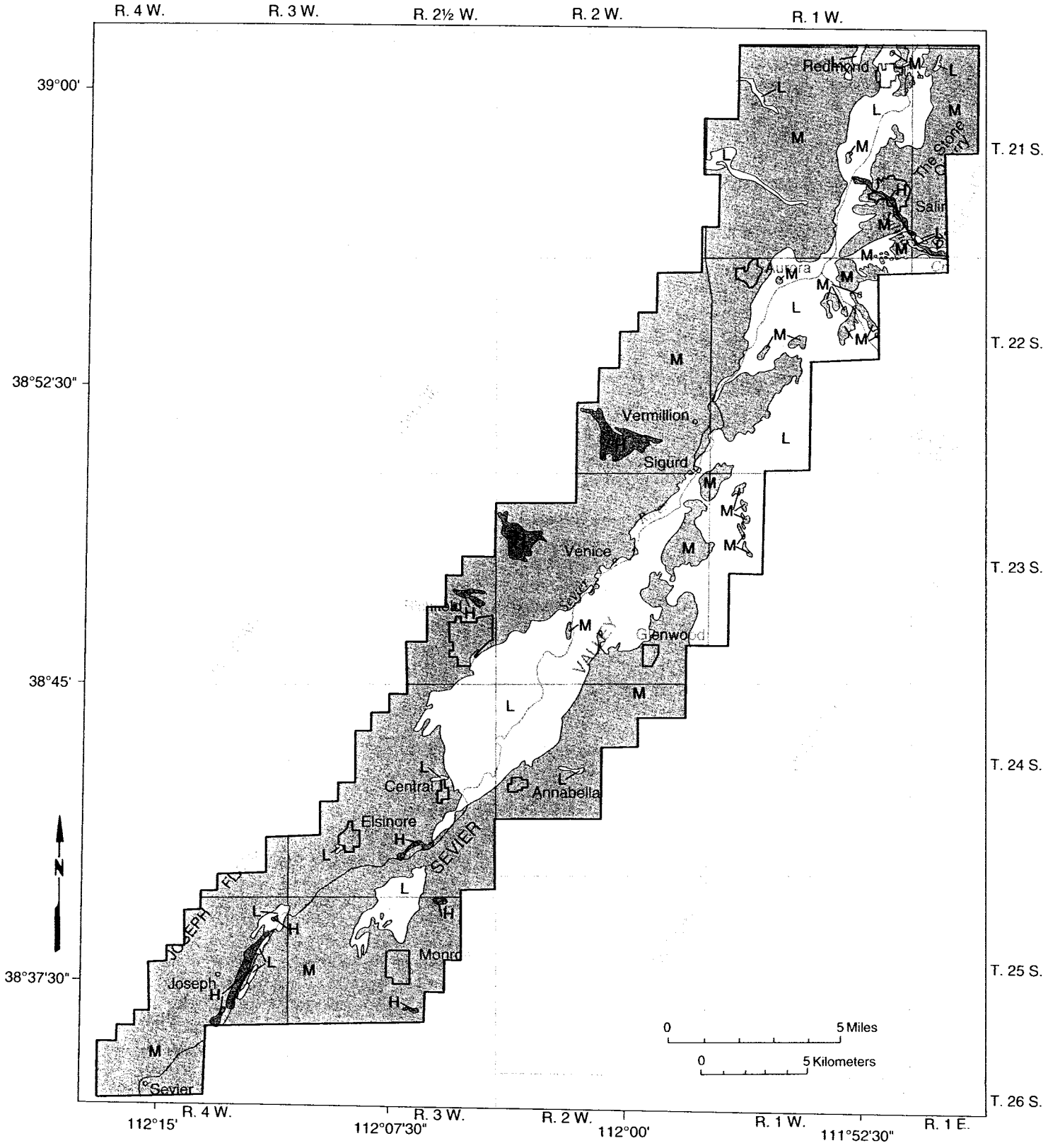

Figure 15. Soil permeability in the central Sevier Valley. L - low, K (hydraulic conductivity) = 0.06 to 0.6 inches/hour (4.2×10^{-5} to 4.2×10^{-4} cm/sec); M - moderate, K = 0.6 to 6.0 inches/hour (4.2×10^{-4} to 4.2×10^{-3} cm/sec); and H - high, K = 6.0 to 20.0 inches/hour (4.2×10^{-3} to 1.4×10^{-2} cm/sec). Data from Wilson and others (1958), modified to reflect the greater permeability of sandy clay to gas than to water (Rogers and Nielson, 1990).

the Sevier River floodplain, but poorly sorted in Salina Creek. Fluvial deposits near Joseph are in the vicinity of Tertiary volcanic rocks, and near Salina are in the vicinity of a mixed terrane of volcanic and older sedimentary rocks, but some of the fluvial deposits may be derived from more distant sources. Alluvial-fan deposits consist of poorly to moderately sorted mixtures of boulders, cobbles, gravel, sand, silt, and clay. Alluvial-fan deposits on the flanks of the Pahvant Range are locally derived from carbonates of the Flagstaff Formation in their drainage basins.

The predominant permeability of soil in the central Sevier Valley is moderate to low. Permeability is moderate in the southern end of the valley in alluvium containing abundant volcanic detritus; on the western side of the valley in alluvium on the flanks of the Pahvant Range derived from volcanic, carbonate, and coarse-grained, clastic sedimentary rocks; and in similar terrane on the eastern valley margin. Soils of low permeability are common near the northeastern valley margin north of Glenwood, and in the Sevier Valley floodplain north of Vermillion, between Sigurd and Annabella, and in scattered areas south of Annabella. North of Glenwood, impermeable soil near the valley margin is locally derived, and in some places residuum, from fine-grained rock of the Arapien Shale. In the Sevier Valley floodplain, impermeable soil is in marshy areas of shallow ground water where springs and seeps are common.

Soil-Gas Radon

The mean concentration of radon in soil gas at 99 sample sites in the central Sevier Valley is 240 pCi/L (8.88 x 10^3 Bq/m^3) (table 1). Distribution of soil-gas radon concentration is approximately lognormal, with a large positive skewness (figure 16). In general, as uranium concentrations increase, radon levels also increase (figure 17). Linear regression of radon-uranium data pairs shows that they are related by the formula:

Eq. 1 $Rn = 29.2U + 136.1$ where:
Rn = the concentration of radon in pCi/L.
U = the concentration of uranium in ppm.

Spearman's rank correlation coefficient, a nonparametric measure of correlation between two variables that are not normally distributed, is 0.374 for this relationship (table 2). At the 99 percent confidence level, the coefficient exceeds the critical value of 0.235, indicating that the correlation between radon and uranium established by linear regression is statistically significant. The critical value was approximated from the relationship of Conover (1980):

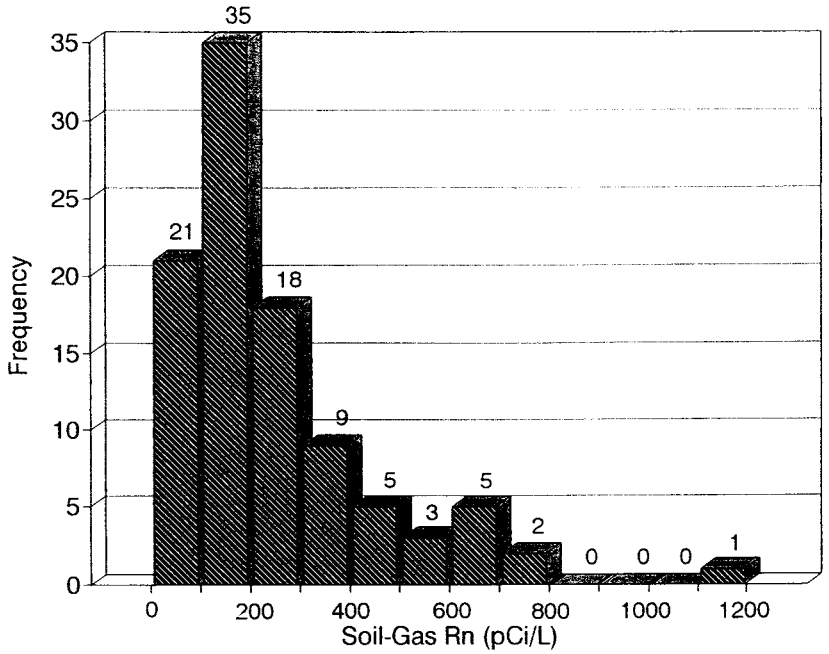

Figure 16. *Histogram of soil-gas-radon concentrations in the central Sevier Valley. Distribution is approximately lognormal, with a large positive skewness. Lognormal distribution is expected when trace elements are randomly distributed in a homogenous material (Rogers, 1964).*

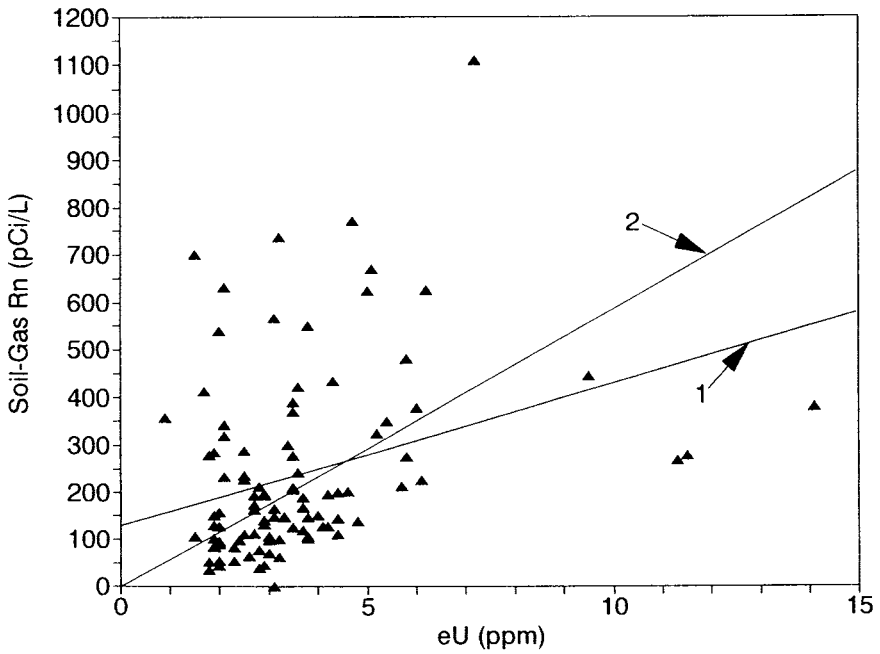

Figure 17. *Scatter plot and linear regression of uranium (U) and soil-gas-radon (Rn) data pairs in the central Sevier Valley. When the regression line (1) is not forced to 0, concentrations are related by the formula Rn = 29.2 U + 136.1, with a Spearman's rank correlation coefficient of 0.374. When the regression line (2) is forced to 0, concentrations are related by the formula Rn = 57.7 U.*

Table 2. Matrix of Spearman's rank correlation coefficients for radiometric data from the central Sevier Valley. All coefficients exceed their respective critical values at the 99 percent confidence level, indicating that direct correlations between data pairs are statistically significant. The critical value for data pairs without soil-gas radon data (sample size 202) is 0.164; the critical value for data pairs with soil-gas radon data (sample size 99) is 0.235. K - potassium-40, eU - equivalent uranium-238, eTh - equivalent thorium-232, Rn - radon-222.

	Total Gamma	K	eU	eTh	Soil-Gas Rn
Total Gamma	1.000	0.965	0.823	0.962	0.429
K	0.965	1.000	0.714	0.907	0.367
eU	0.823	0.714	1.000	0.776	0.374
eTh	0.962	0.907	0.776	1.000	0.463
Soil-Gas Rn	0.429	0.367	0.374	0.463	1.000

Eq. 2 $w_p \approx x_p/(n-1)^{1/2}$ where:
w_p = the critical value of Spearman's rank correlation coefficient.
X_p = the p quantile of a standard normal random variable from Conover (1980, table 1).
n = the sample size.

The correlation coefficient is even greater for the relationships between soil-gas radon and both thorium (0.463) and total gamma (0.429) (table 2). However, a correlation coefficient is only a measure of the strength of the linear relationship between two variables, and does not necessarily imply that a causal relationship exists. In the case of radon and uranium, a causal relationship does exist because ^{222}Rn, the radon isotope measured in this study, is the progeny of the radioactive decay of ^{238}U. Radon and thorium levels correlate well because both uranium and thorium are concentrated in late-stage differentiation of igneous melts (Nielson and others, 1991), and uranium and thorium in the central Sevier Valley are in sediment derived from intermediate to silicic volcanic rocks. High thorium levels, however, are not the cause of high levels of ^{222}Rn. Radon and total gamma levels correlate well because total gamma levels include measurement of elements within a broad radiometric spectrum of which the two most significant components are uranium and thorium.

Soil-gas radon concentrations determined by equation 1 compare favorably with those from other studies in Utah. An eU concentration of 2 ppm in the central Sevier Valley yields a soil-gas radon concentration of 195 pCi/L (7.22×10^3 Bq/m^3) from this relationship. The same eU concentration would yield 113 pCi/L (4.18×10^3 Bq/m^3) in the St. George basin of southwestern Utah (Solomon, 1992) and 187 pCi/L (6.92×10^3 Bq/m^3) in the Weber River area of northern Utah (Black and Solomon, in preparation) from similar relationships. However, Utah radon values appear low when compared to those from similar relationships elsewhere. For example, a uranium concentration of 2 ppm in the Rincon Shale of southern California yields a soil-gas radon concentration in excess of 600 pCi/L (2×10^4 Bq/m^3) (Carlisle and Azzouz, 1991). Ground-water depth and soil permeability contribute to this difference, but climate and soil moisture have more profound effects that are both perennial and seasonal.

Semiarid areas such as the central Sevier Valley are characterized by perennially low soil moisture. Levels of iron oxidation and organic-matter concentration are low in these areas, particularly below the depth of water infiltration (Gundersen and others, 1993). Iron oxides and organic matter are adsorbants of uranium and in semiarid areas are more abundant in thin, shallow soil horizons where uranium levels are measured, but deficient at depths where radon levels are measured. This condition of disequilibrium results in relatively low levels of soil-gas radon even in areas where high uranium concentrations are measured.

Although the average soil moisture is perennially low in semiarid regions, large seasonal variations occur. This results in concurrent seasonal variations in soil-gas radon levels. In a study of radon in a semiarid area of Colorado, soil-gas radon levels were found to vary seasonally by a factor of five or six, with lowest levels during the summer and fall (Asher-Bolinder and others, 1990). This seasonal variation is due to the increased insolation in spring and summer which warms and dries the soil, limiting the amount of water infiltration. Soil normally has enough water to absorb the kinetic energy of radon ions recoiling from the decay of radium, the immediate precursor to radon in the uranium-decay series, so that radon ejected into the pores tends to remain in the pores and is free to move (Tanner, 1989). The fraction of radon atoms which escapes from the solid from which it formed is defined as the emanating power of the solid. As the soil dries, radon emanation decreases, deep soil cracks develop, and convective transport of soil gas increases radon flux into the atmosphere. The concentration of radon in soil gas is concurrently lowered (Asher-Bolinder and others, 1990). The effects of soil cracks are greatest in soils of low permeability (Holford and others, 1993). The addition of a relatively small amount of moisture to expansive clays causes swelling and rapid changes in soil permeability. These rapid changes are a more exaggerated response to moisture input than occurs in soils of different composition (Schumann and others, 1992). Because field work in the central Sevier Valley was conducted during the late summer and early fall, soil-gas radon levels were minimal and may be more comparable to higher levels measured elsewhere had field work in the central Sevier Valley been conducted in other seasons.

The ideal correlation between soil-gas-radon and surface-uranium concentrations measured at the same sites is linear, with a regression line starting at the origin. Because radon is a decay product of uranium, for each unit of uranium that decays a unit of radon should form, and no radon can form in the absence of uranium. In the central Sevier Valley, the correlation, although statistically significant, is imperfect; the relationship is not perfectly linear, nor does the regression line originate at zero (figure 17). If the regression is forced to zero, the data pairs are related

by the formula Rn = 57.7U. Although theoretically ideal, a regression forced to zero does not correctly characterize the data.

Nonlinearity and a non-zero origin are primarily due to three factors: (1) disequilibrium between surficial material tested for uranium and material at shallow depth tested for soil-gas radon, (2) atmospheric contamination of soil-gas samples in permeable soils, and (3) inadequate sample volume in impermeable soils. The effects of these factors are evident in the central Sevier Valley by the presence of several data pairs with high uranium concentrations but low radon concentrations (figure 17), and isolated low radon concentrations in areas of otherwise high levels, such as near Annabella and Joseph (figure 18). Disequilibrium may result from soil-moisture conditions related to the climatic factor noted previously, importation of topsoil or fill in developed areas, or use of fertilizer in agricultural areas. Whereas the climatic factor may cause relatively low levels of soil-gas radon even in areas where high uranium concentrations are measured, the effect of topsoil or fill importation will be based on the differential between the uranium content of imported and native material; fertilizer often has higher uranium levels associated with phosphates, which will make levels of soil-gas radon appear artificially low. Atmospheric contamination may result from air leakage at the interface between the probe and surrounding permeable soils. Tanner (1991b) designed a soil-gas sampling apparatus which, with the use of rubber packers and pressure differentials, minimizes the potential for atmospheric contamination. Clay-rich impermeable soils, particularly if moist, provide a better seal to prevent atmospheric contamination but also, if sufficiently impermeable, plug the probe perforations and prevent sampling. Both atmospheric contamination and probe pluggage cause artificially low soil-gas concentrations, from sample dilution in the first case and inadequate sample volume in the second.

A semiquantitative interpretation method, originally developed for analysis of radon concentrations measured during surface-water surveys (Durrance, 1978), is applied to soil-gas data from the central Sevier Valley to minimize the influence of these factors. The method assumes that these factors can act to reduce the radon concentration of a sample, but only the influx of radon will give rise to high concentrations. If an area of uniformly high radon input is considered, the results of a survey in which sample points have an irregular distribution will show an apparently random pattern of high and low values, the high values being the true indicators and the low values merely being the result of factors which produce artificially low concentrations. It may be inferred, therefore, that only the high values have significance. Instead of constructing contour lines of equal value as shown in figure 18, exclusion isolines are constructed which enclose all data points that have values equal to or greater than the value of the isoline. Areas of consistently high concentrations may then be taken as geologically meaningful. The distribution of areas with high concentrations of soil-gas radon is shown on figure 19.

Soil-gas-radon levels in the central Sevier Valley are commonly high, in excess of 200 pCi/L (7.4 x 10^3 Bq/m^3), in three areas. The largest area of radon-enriched basin fill is along the southern and southeastern valley margins, from Glenwood southward, where the maximum level for this study of 1,108 pCi/L (4.10 x 10^4 Bq/m^3) was measured about 1.5 miles (2.4 km) west of Monroe (figure 19). In this area, Quaternary alluvial-fan and floodplain deposits are locally derived from uraniferous volcanic rocks in adjacent mountains. Two smaller areas of radon-enriched basin fill are in the Sevier River floodplain, one west of Glenwood where radon levels are as high as 565 pCi/L (2.09 x 10^4 Bq/m^3), and the other west of Salina where radon levels are as high as 770 pCi/L (2.85 x 10^4 Bq/m^3). The source of uraniferous sediment is more ambiguous in the floodplain, but sediment is at least partly derived from local and upstream volcanic material. Moderate levels of radon, between 100 and 200 pCi/L (3.7 x 10^3 and 7.4 x 10^3 Bq/m^3), were recorded on the western valley margin and adjacent Sevier River floodplain, near Aurora and Sigurd and between Joseph and Richfield. Volcanic rocks are present near the former area, but floodplain deposits probably include a significant component of less uraniferous sediment from a more distant source. Uranium-deficient, pre-volcanic sedimentary rocks are present near the latter area. The lowest levels of soil-gas radon, where concentrations were routinely less than 100 pCi/L (3.7 x 10^3 Bq/m^3), are in four small areas in the northern part of the study area: (1) north of Richfield, (2) between Glenwood and Sigurd, (3) southwest of Salina, and (4) west of Redmond. All of these areas are underlain by Quaternary alluvium derived from adjacent outcrops of uranium-deficient, pre-volcanic sedimentary rocks.

Indoor Radon

Geologic factors influence radon levels in soil gas, but a number of non-geologic factors also influence radon levels once the gas enters the construction zone and migrates indoors. Significant non-geologic factors include foundation condition, building ventilation, construction material, and life styles (Fleischer and others, 1982). The distribution of indoor-radon levels reflects the combined influence of both geologic and non-geologic factors.

Thirty-eight residential indoor-radon levels were measured in the central Sevier Valley (Solomon and others, 1993) (appendix table A-2). The measurements average 4.9 pCi/L (181.3 Bq/m^3)(table 1), with 44 percent greater than or equal to 4 pCi/L (148 Bq/m^3)(table 3). Average levels of indoor radon in the central Sevier Valley are considerably greater than average levels in Utah and the United States. The statewide average indoor-radon level is 2.7 pCi/L (100 Bq/m^3) (figure 20), with 16 percent greater than or equal to 4 pCi/L (148 Bq/m^3) (Solomon and others, 1993). Comparable figures for the United States are an average of 1.7 pCi/L (63 Bq/m^3), with 6 percent greater than or equal to 4 pCi/L (148 Bq/m^3) (Sextro, 1988).

Four measurements greater than or equal to 10 pCi/L (370 Bq/m^3) were recorded in the central Sevier Valley. All four measurements, with a maximum of 22.4 pCi/L (828.8 Bq/m^3), are clustered within an area of about 1 square mile (2.6 km^2) on the southern margin of Monroe (figure 21). This area is underlain by well-drained, moderately permeable alluvium derived from adjacent uraniferous volcanic rocks. Elevated, yet more moderate, indoor measurements of between 4 and 10 pCi/L (148 and 370 Bq/m^3) are scattered throughout the central and southern parts of the valley from Venice southward, where uraniferous

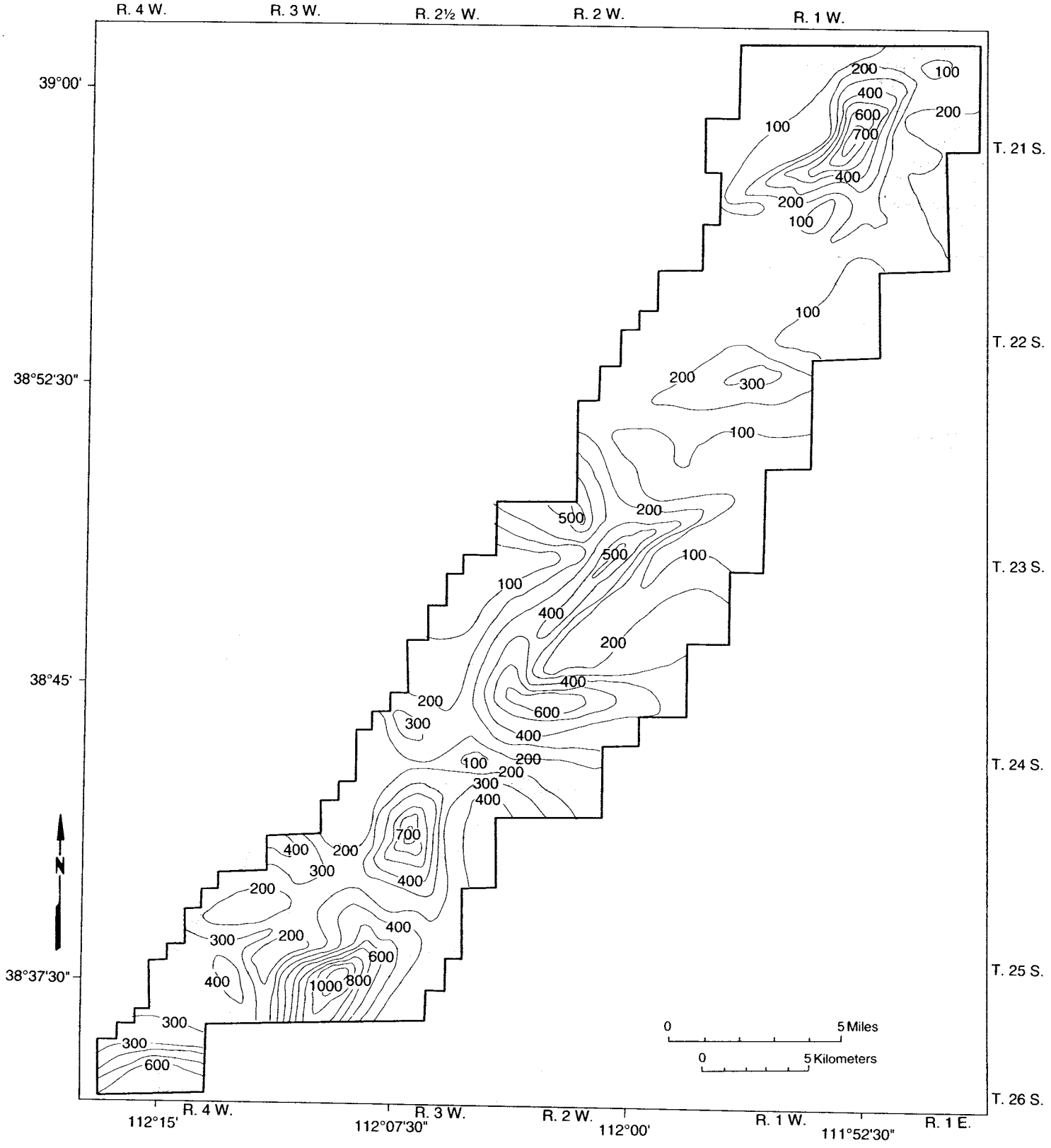

Figure 18. Soil-gas-radon concentrations in the central Sevier Valley. Contour interval is 100 pCi/L (3.7 x 10^3 Bq/m^3).

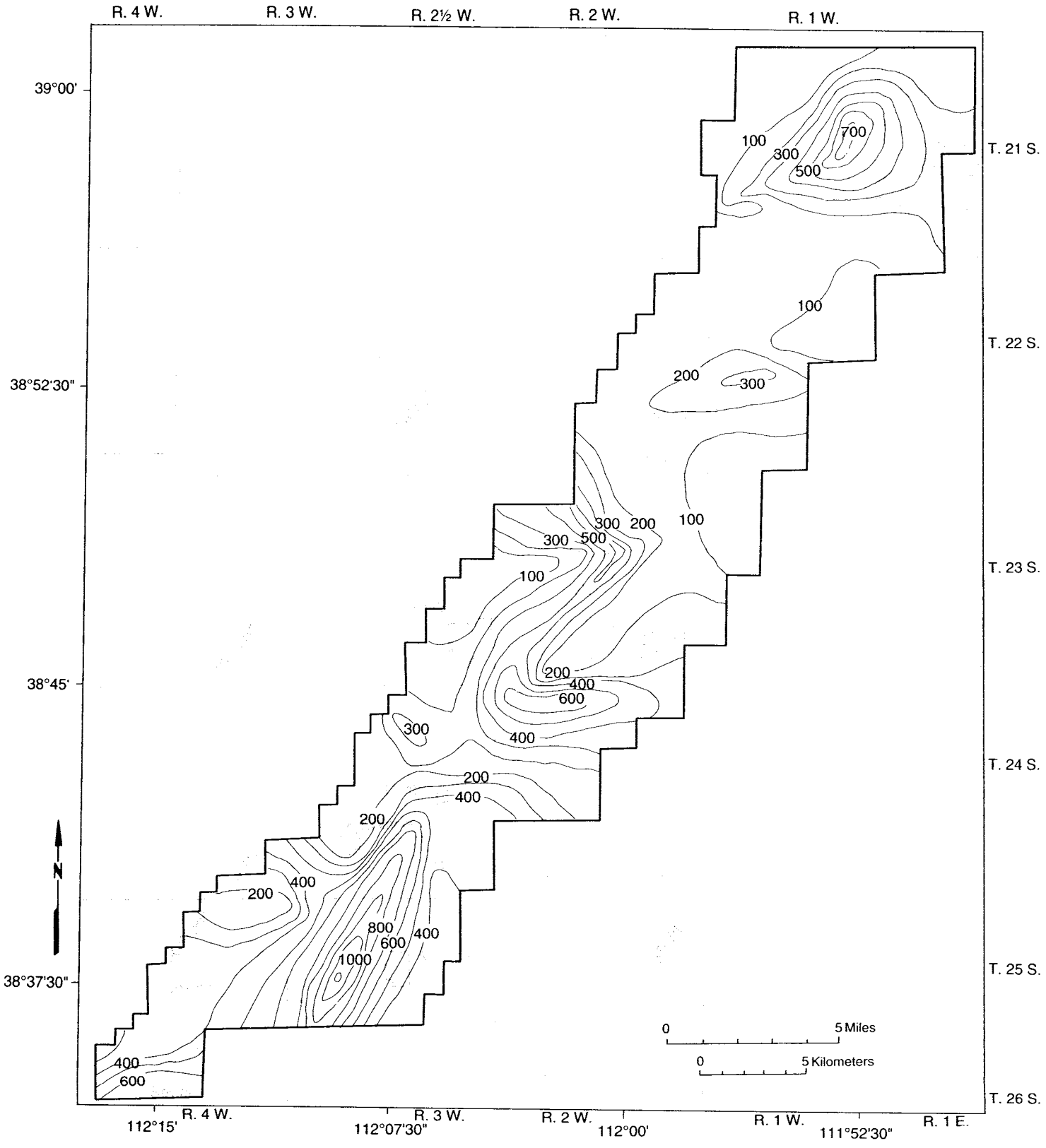

Figure 19. Exclusion isolines of soil-gas-radon concentrations in the central Sevier Valley. Exclusion isolines enclose all data points with values equal to or greater than the value of the isoline. Contour interval is 100 pCi/L (3.7 x 10^3 Bq/m^3).

Table 3. Residential indoor-radon concentrations in the central Sevier Valley (this study) and Utah (Solomon and others, 1993). The average concentration is significantly larger in the central Sevier Valley, where concentrations are skewed towards higher values. The comparative distribution of local and statewide indoor concentrations is graphically illustrated in figure 20. N - number of samples in the specified range of indoor-radon concentrations.

Area		Central Sevier Valley	Utah
Sample Size		38	1,133
Minimum		0.3	0.0
Median		4.9	2.7
Maximum		22.4	68.2
<4 pCi/L	N	21	954
	%	55	84
4<10 pCi/L	N	13	145
	%	34	13
10<20 pCi/L	N	2	27
	%	5	2
≥20 pCi/L	N	2	7
	%	5	1

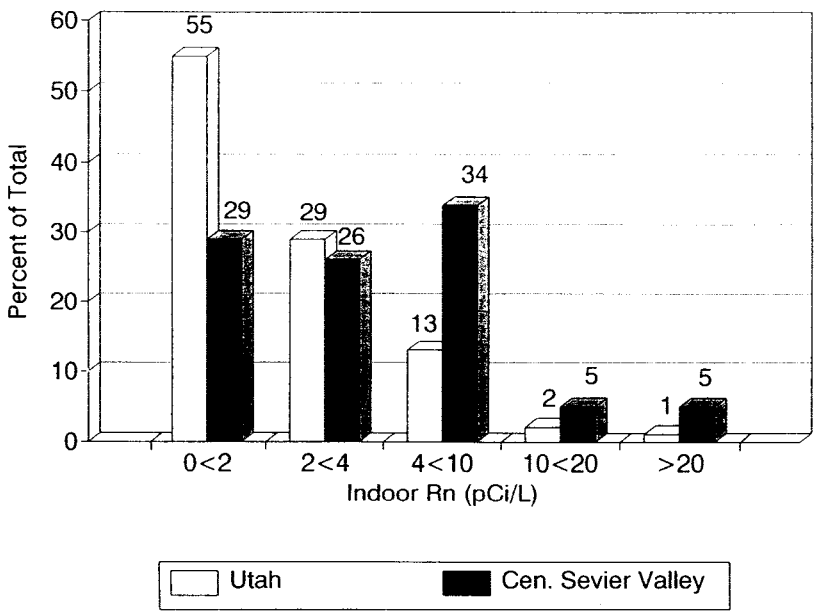

Figure 20. Comparison of residential indoor-radon concentrations in Utah and the central Sevier Valley. Statewide data modified from Solomon and others (1993).

volcanic detritus is more common. Several of these measurements are clustered in western and southern Richfield. The northern part of Richfield, where indoor-radon levels are commonly less than 4 pCi/L (148 Bq/m^3), is underlain by alluvium derived from Tertiary sedimentary rocks with low uranium concentrations. Indoor-radon levels less than 4 pCi/L (148 Bq/m^3) are also prevalent elsewhere in the northern part of the valley where uranium levels are generally low, ground water is shallow, and soil is less permeable. Alluvium in the northern part of the valley is commonly derived from pre-volcanic sedimentary rocks with low concentrations of uranium.

Low levels of radon were measured in the three schools in the central Sevier Valley sampled for this study (figure 21) (appendix table A-3). The only school radon measurement greater than 4 pCi/L (148 Bq/m^3) was 5.1 pCi/L (188.7 Bq/m^3) in a kitchen storeroom at South Sevier High School (table 4), but 14 other measurements throughout the school were less than 4 pCi/L (148 Bq/m^3). Of the three schools, this one is closest to the cluster of residential measurements greater than 10 pCi/L (370 Bq/m^3) in southern Monroe. Both this school and South Sevier Middle School, where a maximum measurement of 2.8 pCi/L (103.6 Bq/m^3) was recorded, are in the vicinity of residential measurements in Monroe between 4 and 10 pCi/L (148 and 370 Bq/m^3), but lower residential measurements were recorded within 0.5 miles (0.8 km) of each school. A maximum measurement of 0.4 pCi/L (14.8 Bq/m^3) was recorded at Ashman Elementary School in western Richfield, within 0.5 miles (0.8 km) of seven residential measurements ranging from 0.3 to 6.8 pCi/L (11.1 to 251.6 Bq/m^3). Because construction techniques and use of homes and schools differ considerably, indoor-radon levels in these building types are not directly comparable, but measurements in schools are not inconsistent with nearby residential measurements.

Other Radiometric Measurements

Whereas gamma-ray measurements of equivalent uranium can be used to estimate the relative amounts of radon in soil gas, gamma-ray measurements of other elements are useful for the geologic interpretation of uranium and additional factors related to the indoor-radon hazard. Both the element concentrations and ratios between elements contain patterns related to the lithology of source rocks that govern the distribution of radon in valley fill. Ratio maps can also indicate anomalous concentrations of the elemental components of the ratio because radioelement concentrations vary both with lithology and within lithologic units, and lithologic differences tend to be removed (Duval, 1983). Other data collected during the ground gamma-ray survey include measurements of K, eTh, and total gamma (table A-1).

Higher K concentrations are generally coincident with uraniferous volcanic detritus in the central Sevier Valley, and are most com-

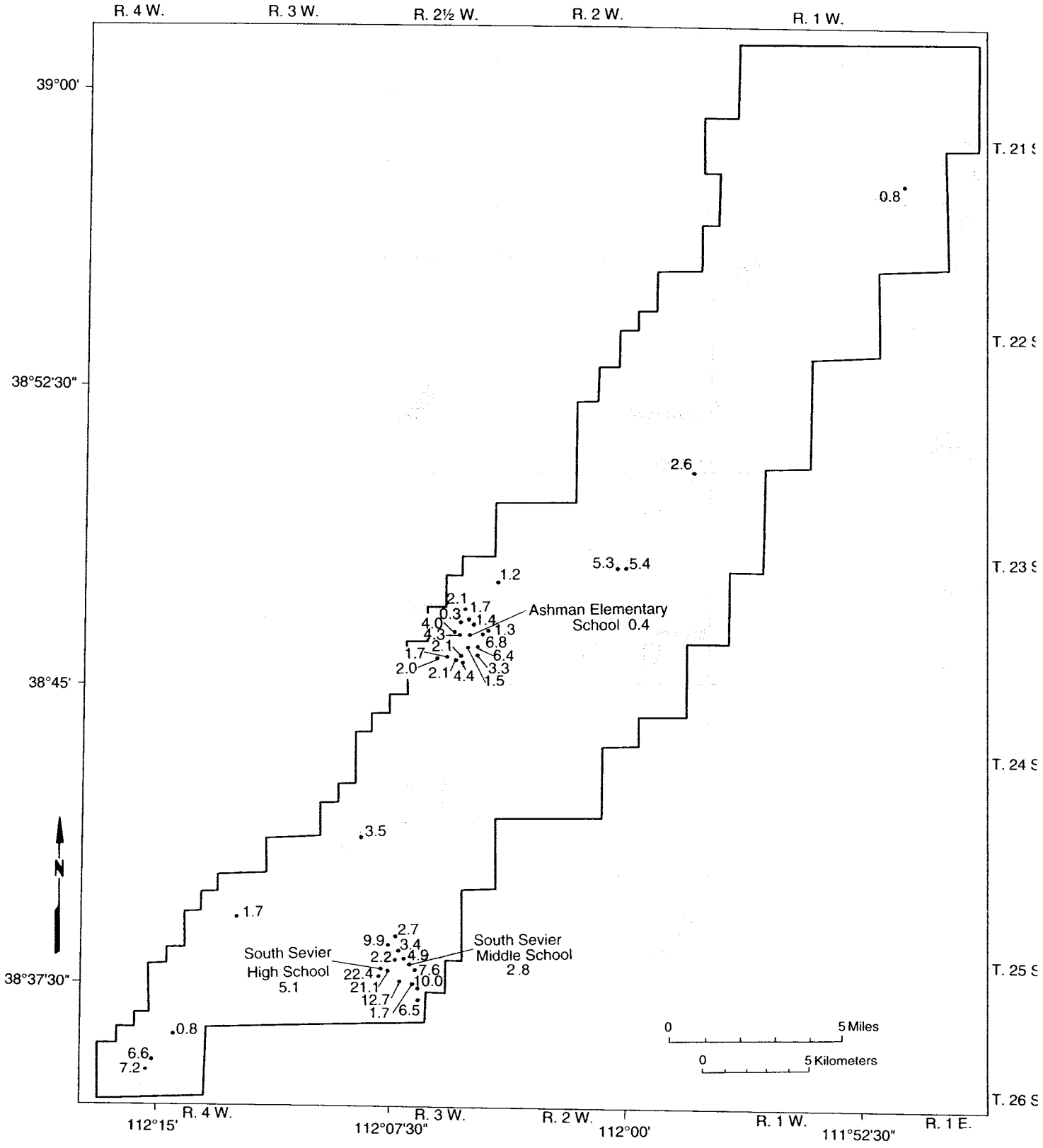

Figure 21. *Indoor-radon concentrations, in pCi/L, in the central Sevier Valley. The level of indoor radon was measured in several locations in the three schools sampled for this study (see table 4 and appendix table A-3), but only the highest of these measurements in each school are shown.*

Table 4. School indoor-radon concentrations in the central Sevier Valley. A hazard-potential category for each school location was determined from the hazard-potential map (figure 30). Tested schools were randomly selected. N - number of samples with an indoor-radon concentration greater than, or equal to, 4 picocuries of radon per liter of air (148 Bq/m^3).

Location	Sample Size	Minimum	Median	Maximum	≥4 pCi/L		Hazard Category
					N	%	
Monroe							
Monroe Elementary	0	---	---	---	---	---	Moderate
South Sevier Middle	9	0.1	1.0	2.8	0	0	High
South Sevier High	17	0.2	2.1	5.1	1	6	Moderate
Richfield							
Ashman Elementary	18	0.0	0.1	0.4	0	0	Moderate
Pahvant Elementary	0	---	---	---	---	---	Moderate
Red Hills Middle	0	---	---	---	---	---	Moderate
Richfield High	0	---	---	---	---	---	Moderate
Sevier Valley Tech	0	---	---	---	---	---	High
Salina							
Salina Elementary	0	---	---	---	---	---	Moderate
North Sevier Middle	0	---	---	---	---	---	Moderate
North Sevier High	0	---	---	---	---	---	Moderate

mon in the southern part of the study area. Concentrations of K have an approximately normal distribution (figure 22), common for chemical constituents of soils with mean values in the range of 1 to 10 percent (Sinclair, 1986). The mean concentration of K in the central Sevier Valley is 1.9 percent, with a maximum of 4.4 percent measured east of Salina in alluvium near an outcrop of Osiris Tuff (table 1).

Concentrations of K and eU are linearly related if eU concentrations, with an approximately lognormal distribution (figure 23), are plotted on a logarithmic scale. Spearman's rank correlation coefficient is 0.714 for this relationship (table 2), which exceeds the critical value of 0.164 at the 99 percent confidence level. The correlation coefficient is even higher for linear relationships between K and both thorium (0.907) and total gamma (0.962). All three relationships are consistent with concentration of these elements in silicic volcanic rocks. From Elsinore southward, where volcanic rock is predominant on valley margins, K concentrations are typically between 2 and 4 percent, and eU concentrations are typically between 3 and 9 ppm; from Venice northward where pre-volcanic sedimentary rock is predominant on valley margins, K concentrations are typically less than 3 percent, and eU concentrations are typically less than 3 ppm.

The largest ratios of eU and K are associated with different concentrations of eU in the two areas. Values for eU/K are greater than 2 in the south where eU concentrations are typically greater than 5 ppm, but similar ratio values in the north are associated with eU concentrations typically between 2 and 4 ppm. Determination of anomalous K concentrations is beyond the scope of this report, and maps of K concentrations and eU/K ratios are therefore not provided.

Although the indoor-radon hazard is primarily controlled by the concentration of ^{238}U in foundation soil and reflected by the concentration of ^{222}Rn in indoor air, houses built on soil enriched in ^{232}Th may be subject to a hazard from its ^{220}Rn daughter. The half-life of ^{220}Rn is 54.5 seconds, much shorter than the 3.82-day half-life of ^{222}Rn, but in sufficient quantities the α-energy concentration of ^{220}Rn daughters may be much higher than that of ^{222}Rn daughters (Stranden, 1984). Concentrations of ^{232}Th (eTh) in the central Sevier Valley have an approximately lognormal distribution (figure 24). The mean concentration of eTh is 11.1 ppm, with a maximum of 41.9 ppm measured east of Salina where the maximum K concentration was recorded (table 1).

Concentrations of eTh and eU are linearly related (figure 25), and the Spearman's rank correlation coefficient of 0.776 for this

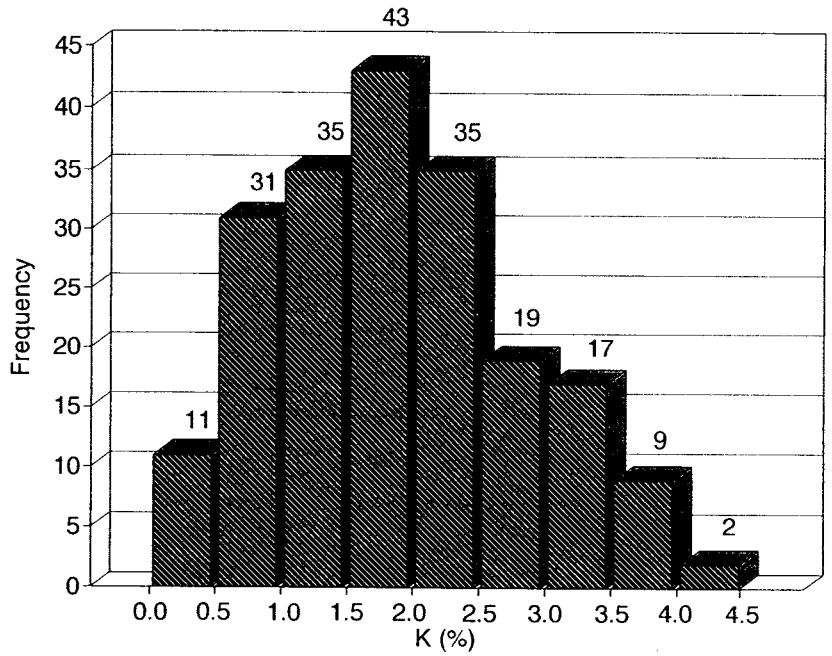

Figure 22. Histogram of potassium concentrations in the central Sevier Valley. Distribution is approximately normal, common for chemical constituents of soils with mean values in the range of 1 to 10 percent (Sinclair, 1986).

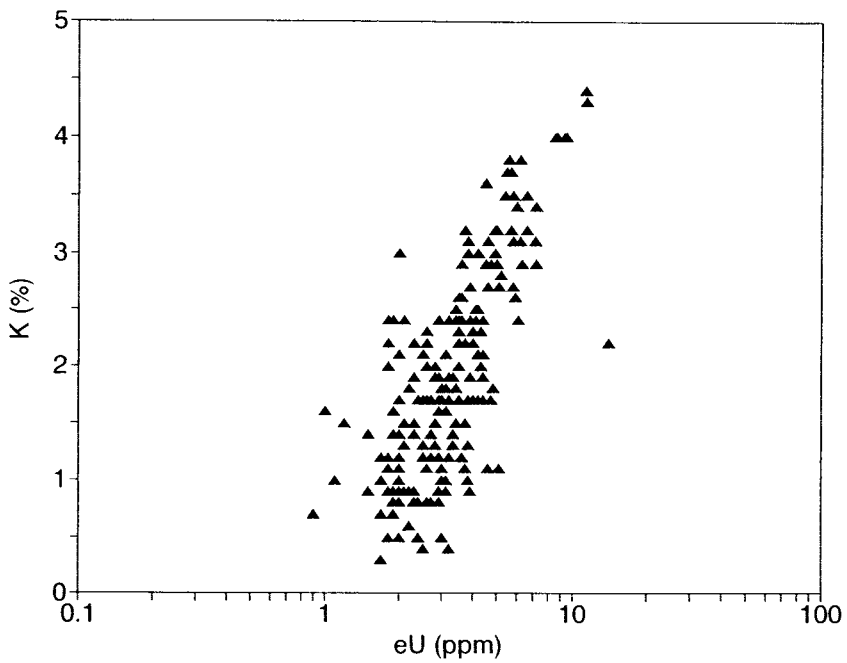

Figure 23. Scatter plot of uranium and potassium data pairs in the central Sevier Valley. The Spearman's rank correlation coefficient of 0.714 exceeds the critical value of 0.164 at the 99 percent confidence level.

relationship (table 2) exceeds the critical value of 0.164 at the 99 percent confidence level. The correlation coefficient is even higher for linear relationships between eTh and both K (0.907) and total gamma (0.962). All three relationships are consistent with concentration of these elements in silicic volcanic rocks. From Elsinore southward, and along the northeastern valley margin, eTh concentrations are typically greater than 10 ppm; from Venice northward, along the northwestern valley margin, eTh concentrations are typically smaller (figure 26).

Ratios of eU and eTh greater than 0.5 are commonly associated with alluvial-fan deposits locally derived from uranium- and thorium-deficient rocks of the Flagstaff and Green River Formations on the northwestern valley margin (figure 27). Basin-fill deposits locally derived from volcanic rocks typically have eU/eTh ratios less than 0.5. The persistence of relatively constant ratio values in Quaternary deposits near particular geologic units suggests that the ratios are strongly influenced by source-rock chemistry, rather than by preferential leaching of soluble uranium under oxidizing conditions. However, an exceptionally high ratio of 1.18 is associated with travertine at Red Hill Hot Springs. This high ratio, and the anomalously low concentration of associated thorium (figure 26), suggests uranium enrichment of the travertine from circulation of mineralized thermal water, possibly enhanced by leaching of uranium from the travertine after deposition. Uranium is soluble under the oxidizing conditions of shallow soil and is readily leached. Daughter products, however, are not leached. One daughter product, ^{214}Bi, has a more distinctive spectral peak than ^{238}U and it is this bismuth isotope that is actually measured during a spectrographic survey. The amount of measured ^{214}Bi is converted to an equivalent concentration of the parent uranium (eU), and uranium is thus overestimated in the radiometric analysis (Nielson and others, 1991).

Total gamma count represents a broad spectrum of gamma radiation that is converted to an equivalent concentration of ^{238}U. Concentrations of total gamma have an approximately lognormal distribution, with multiple secon-

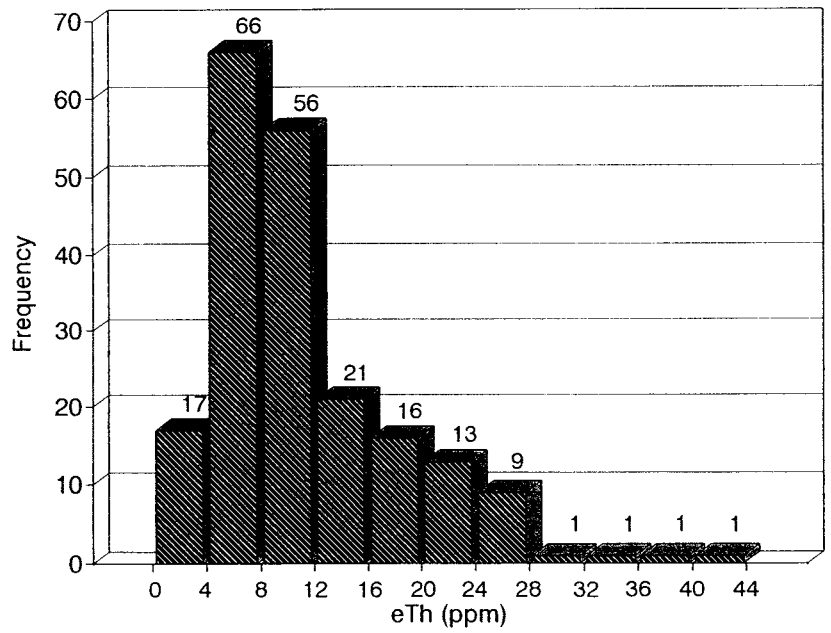

Figure 24. Histogram of thorium concentrations in the central Sevier Valley. Distribution is approximately lognormal, with a moderate positive skewness. Lognormal distribution is expected when trace elements are randomly distributed in a homogenous material (Rogers, 1964).

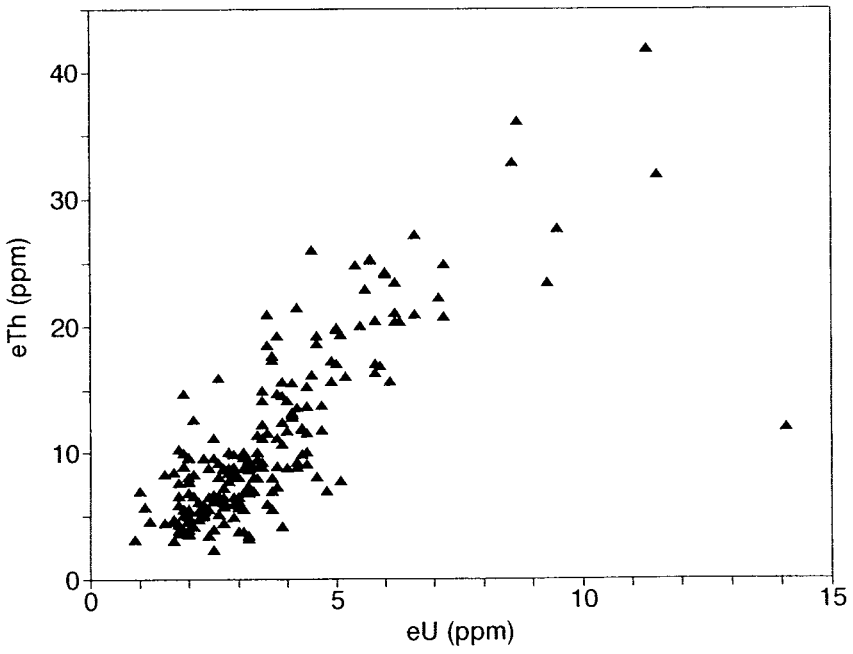

Figure 25. Scatter plot of uranium and thorium data pairs in the central Sevier Valley. The Spearman's rank correlation coefficient of 0.776 exceeds the critical value of 0.164 at the 99 percent confidence level.

dary modes representing different spectral constituents (figure 28). The mean concentration of total gamma in the central Sevier Valley is 14.3 ppm, with a maximum of 43.5 ppm measured east of Salina where the maximum K and eTh concentrations were recorded (table 1).

Spearman's rank correlation coefficients for the linear relationships between total gamma concentrations and eU, eTh, and K concentrations are respectively 0.823, 0.962, and 0.965 (table 2). All exceed the critical value of 0.164 at the 99 percent confidence level and indicate that the relationships are consistent with concentration of these elements in silicic volcanic rocks. Because of the statistically significant linear correlation between total gamma and eTh (figure 29), and because a map of eTh distribution (figure 26) was constructed to illustrate the potential hazard from ^{220}Rn, a map of total gamma distribution is not provided; eTh distribution likely reflects that of total gamma radiation.

RADON-HAZARD POTENTIAL

Geologic factors which influence indoor-radon levels have been used to classify the relative hazard potential in the central Sevier Valley. Hazard-classification boundaries, independent of mapped geologic units, are compiled on a composite hazard map derived from overlays of rating factors. This system, adapted from Solomon (1992), accommodates a large data set, wide value ranges, and a large study area. The system is not applicable in all settings, but is suitable for a wide variety of radon-hazard assessments. This method of hazard mapping is only one of several possible schemes. Solomon and others (1994), for example, statistically characterize relevant geologic factors within each geologic unit to determine its relative hazard potential. However, this method assumed uniform physical characteristics within geologic units and disregarded inhomogeneities and source-area considerations. Such hazard assessments ignore the nonparametric nature of statistics which commonly characterize the distribution of trace elements in the natural environment, and are biased towards

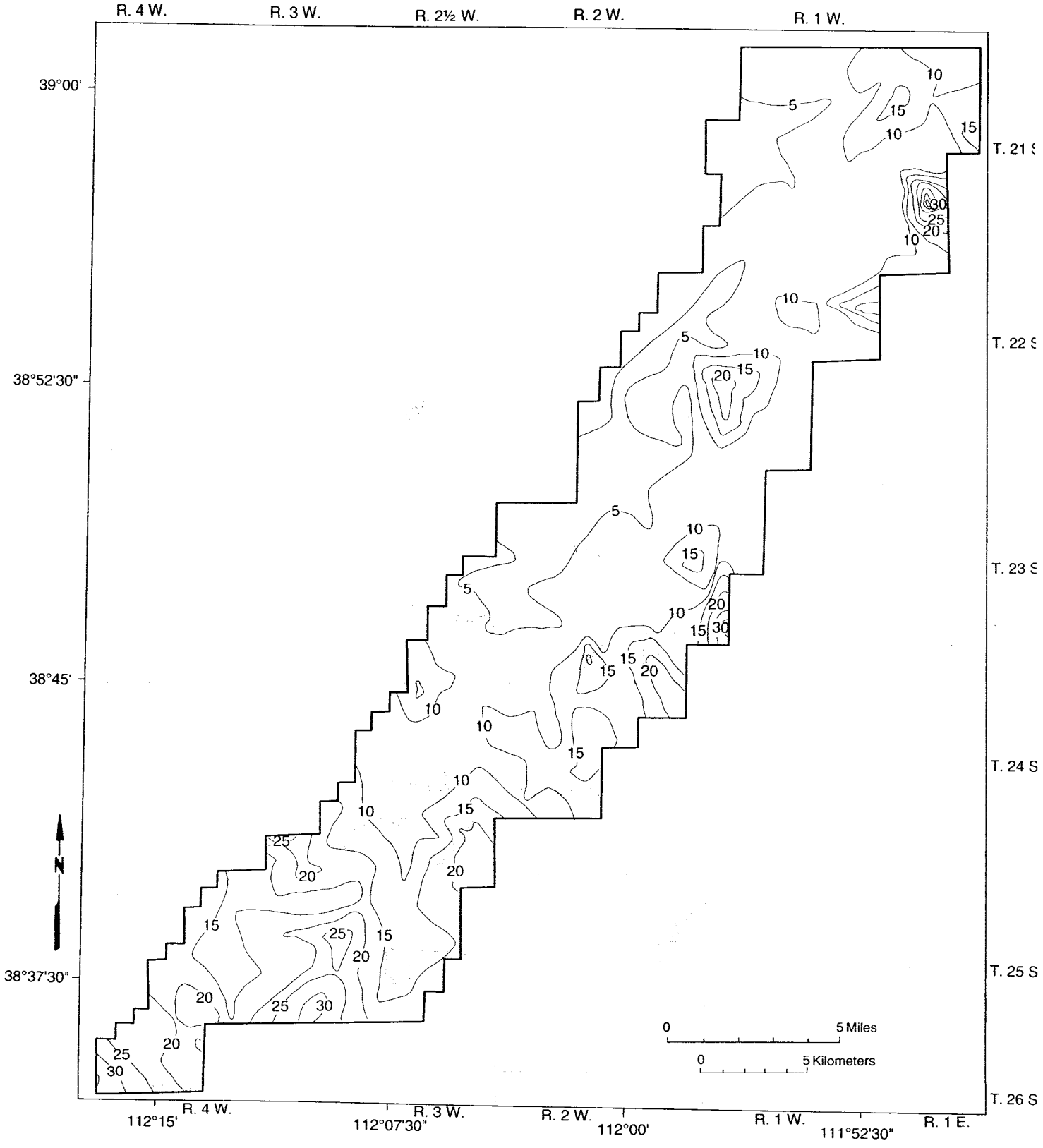

Figure 26. *Thorium (eTh) concentrations from gamma-ray spectrometry in the central Sevier Valley. Contour interval is 1 ppm. Elevated thorium concentrations are common in Quaternary alluvium locally derived from Tertiary rhyolitic tuff.*

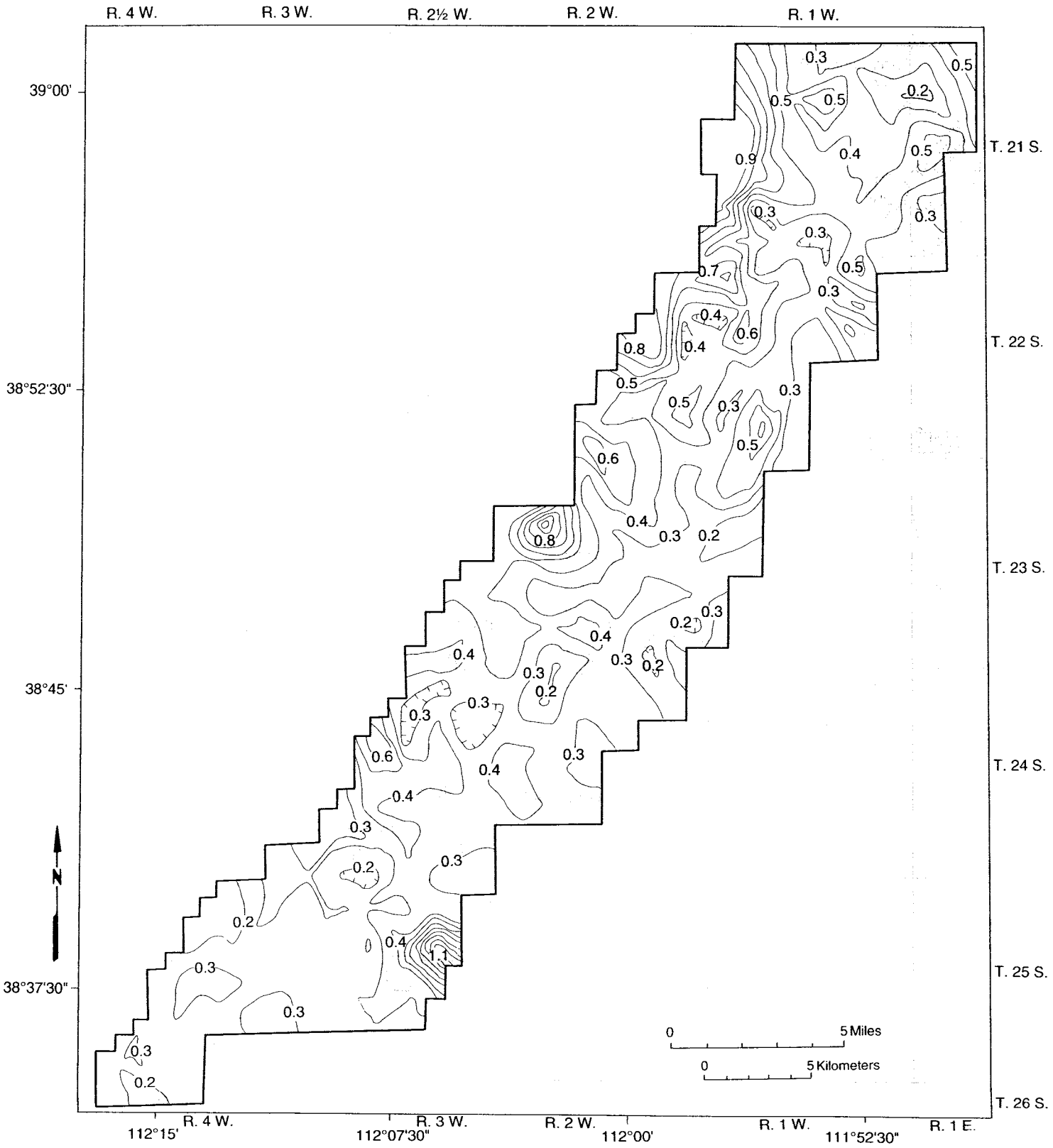

Figure 27. eU/eTh ratios from gamma-ray spectrometry in the central Sevier Valley. Contour interval is 0.1. Basin-fill deposits locally derived from volcanic rocks typically have eU/eTh ratios less than 0.5.

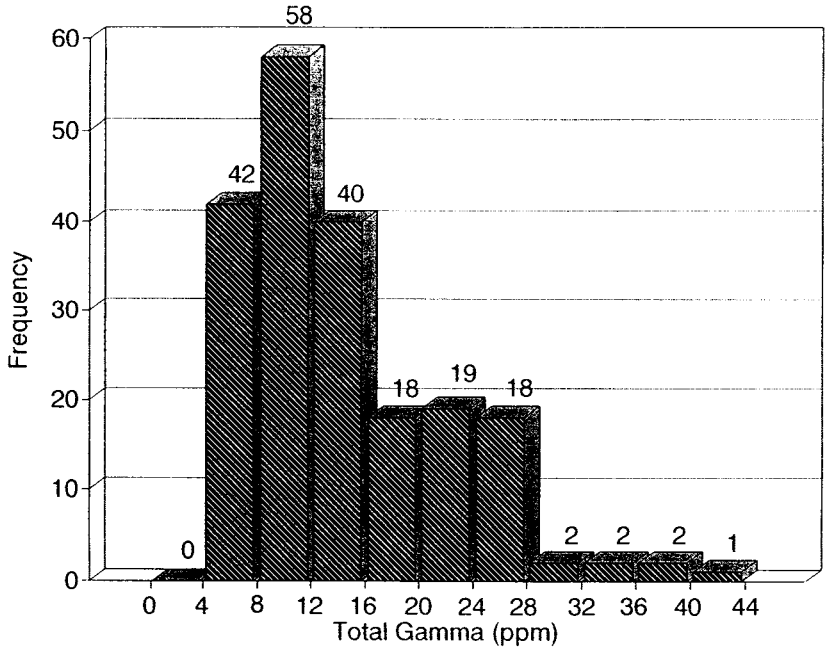

Figure 28. *Histogram of total gamma concentrations in the central Sevier Valley. Distribution reflects the sum of individual constituents measured within a broad spectral range.*

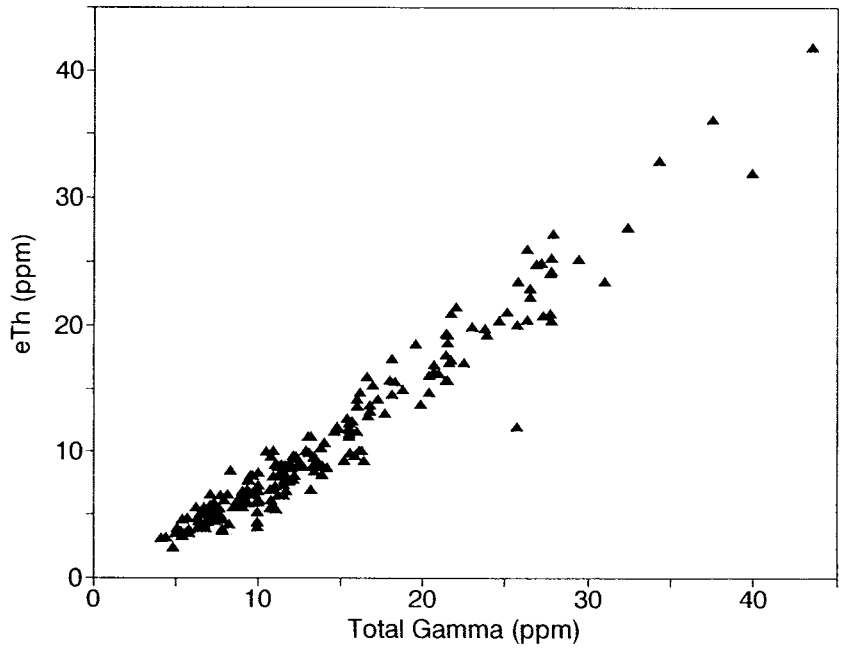

Figure 29. *Scatter plot of total gamma and thorium data pairs in the central Sevier Valley. The Spearman's rank correlation coefficient of 0.962 exceeds the critical value of 0.164 at the 99 percent confidence level. The coefficient approaches unity because thorium is a significant component of total gamma radiation in the measured spectral range.*

geologic factors which may be statistically dominant but of limited areal extent. The EPA summarizes relevant factors within county boundaries to characterize radon-hazard zones (U.S. Environmental Protection Agency, 1993). This method generalized the hazard for political expediency and disregarded inhomogeneities, in this case within political, rather than geologic, units. Sweden established criteria for radon-hazard assessment based on soil-gas radon levels (Akerblom, 1986; Wilson, 1987). Duval (1991) shows that more comprehensive measures of radon availability, as used in this study of the central Sevier Valley, provide more realistic estimates, and demonstrates that the use of inadequate criteria can result in inaccurate assessments of radon-hazard potential.

Numerical ratings from 1 to 3 were assigned to each of the three geologic factors used to evaluate radon-hazard potential in the central Sevier Valley: (1) uranium concentration, (2) soil permeability, and (3) ground-water depth (table 5). Higher ratings correspond to conditions favorable for elevated indoor-radon concentrations. Ratings for the three factors were summed for each area on a composite map derived from overlays of the three factors, and each area was placed within one of three radon-hazard-potential categories based on the cumulative totals of the three factors (table 6). The factors are equally weighted because insufficient data is available to evaluate the sensitivity of radon-hazard-potential categories to individual factors.

Hazard Distribution

The three radon-hazard-potential categories in the central Sevier Valley (figure 30), and their relation to evaluated geologic factors, are: (1) high - areas with geologic factors generally conducive to elevated indoor-radon levels; (2) moderate - areas with one or two factors conducive to elevated indoor-radon levels, but limited by one or two unfavorable geologic conditions; and (3) low - areas with geologic factors generally not conducive

Table 5. Radon-hazard-potential matrix. Soil permeability classes are characterized by hydraulic conductivity, K.

FACTOR	POINT VALUE		
	1	2	3
Uranium (ppm)	<2	2-3	>3
Permeability (K, in/hr)	Low 0.06-0.6	Moderate 0.6-6.0	High 6.0-20.0
Ground-water depth (ft)	<10	10-50	>50

Table 6. Radon-hazard-potential categories. See table 5 for point value of factors in each category.

HAZARD CATEGORY	POINT RANGE	PROBABLE INDOOR-Rn CONCENTRATION (pCi/L)
Low	3-4	<2
Moderate	5-7	2-4
High	8-9	>4

to elevated indoor-radon levels. The radon-hazard potential is controlled by source-rock distribution and the geologic characteristics of derived basin-fill deposits.

The most extensive area of high-hazard potential extends from the southern part of the valley, between Monroe and Sevier, northward along the valley margins to Richfield on the west and Glenwood on the east. Smaller areas of high-hazard potential are present on the western valley margin north and east of Vermillion, and on the eastern valley margin from Salina northward. These areas are characteristically underlain by moderately permeable, well drained, and uraniferous Quaternary alluvial-fan deposits derived from Tertiary volcanic rocks.

Areas of moderate-hazard potential are common in the central part of the valley from Monroe northward, and along the central valley margins from Richfield to Vermillion on the west, and from Glenwood to Salina on the east. These areas are characteristically underlain by moderately permeable, drained, and uraniferous Quaternary alluvial-fan and floodplain deposits derived from a mixture of sources composed predominantly of pre-volcanic sedimentary rocks, but with a significant volcanic component. Ground water in these areas, although commonly too deep to influence radon migration, may seasonally rise to the construction zone and be of significance. A large area south of Redmond underlain by impermeable and poorly drained deposits, conditions not conducive to elevated indoor-radon levels, also is subject to a moderate-hazard potential because of elevated uranium levels.

Areas of low-hazard potential are restricted to the Sevier River floodplain between Annabella and Vermillion, and north of Aurora. These Quaternary floodplain deposits are impermeable and poorly drained, with ground water commonly discharging to the surface where forced upward by adjacent bedrock constrictions. Deposits in areas of low-hazard potential typically have low to moderate uranium levels in material transported by the Sevier River from both distant and local sources.

The radon-hazard potential mapped in this study is similar to that of the central Sevier Valley mapped in the statewide study of radon-hazard potential by Black (1993) (figure 31). In both maps, hazard potential is highest in the vicinity of Tertiary volcanic rocks and lowest in poorly drained areas along the valley axis. Dubiel (1993) divides the state into nine areas of unique geologic characteristics and categorizes the radon-hazard potential of each area. Sevier County occupies parts of two areas, both of which have high radon-hazard potentials. Considering generalizations necessary to accommodate the small-scale map of Dubiel (1993), the hazard potential of the southern part of the county, including the southern part of the central Sevier Valley, generally agrees with the assessment of hazard potential in both Black (1993) and this study. However, the hazard potential of the northern part of both Sevier County and the central Sevier Valley is predominantly moderate in both Black (1993) and this study, as opposed to the high-hazard potential assigned by Dubiel (1993). The EPA (U.S. Environmental Protection Agency, 1993) assigned each county in Utah to one of three radon zones, based on the predominant hazard potential in the county determined by Dubiel (1993). Sevier County is assigned to radon zone 1, the highest hazard-potential zone of the three.

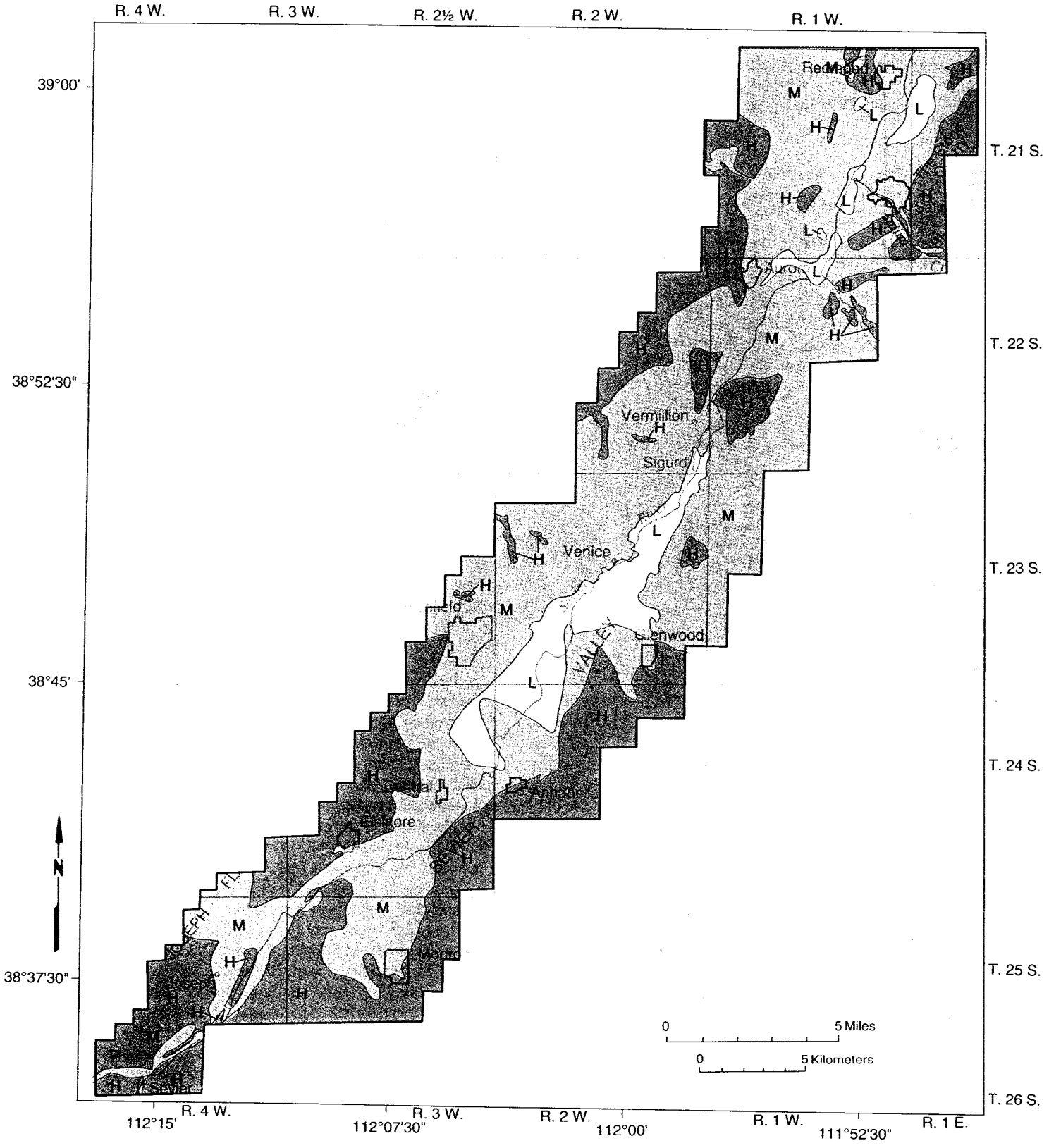

Figure 30. *Indoor-radon-hazard potential of the central Sevier Valley. L (light shading) - low, M (medium shading) - moderate, and H (dark shading) - high. See table 6 for definition of hazard-potential categories.*

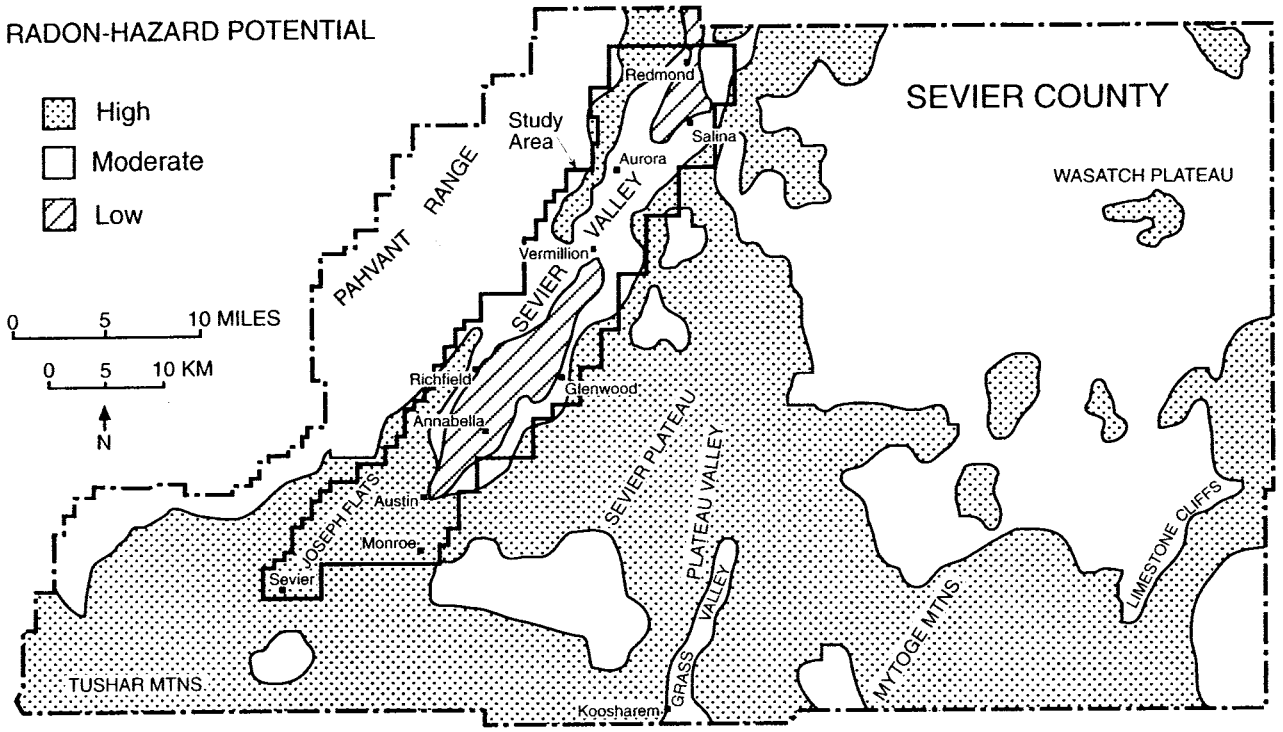

Figure 31. Indoor-radon-hazard potential of Sevier County (modified from Black, 1993). The central Sevier Valley study area is outlined. Radon-hazard potential of this area in the present study (figure 30) is similar to that of Black (1993), with most discrepancies due to the difference in scale between the two investigations.

Hazard Potential and Soil-Gas-Radon Levels

Variations in hazard potential (figure 30) approximate variations in soil-radon levels (figures 18 and 19) in the central Sevier Valley. Low radon levels in the Sevier River floodplain between Glenwood and Vermillion generally coincide with the large area of lowest hazard potential. The area of high radon levels in the southern end of the valley has a predominantly high-hazard potential. There are, however, some inconsistencies in the correlation such as the association of relatively low levels of soil-gas radon with a high-hazard potential on the valley margin west of Aurora and Vermillion. This inconsistency is the result of a statistical inadequacy of the soil-gas sampling grid due to the inability of the probe to penetrate dense alluvial-fan gravels; in this area the soil-gas data are insufficient and both figures 18 and 19 do not accurately reflect the hazard potential. Elsewhere, inconsistencies may be caused by atmospheric contamination of soil-gas samples resulting in low levels of soil-gas radon in high-hazard areas, or the influence of physical phenomena not considered in the hazard evaluation. Unmeasured physical phenomena include meteorological effects (Kraner and others, 1964); changes in ground-water pressure, temperature, fluid solubility, and gas content (Rogers, 1958; Stoker and Kruger, 1975); and the effect of grain size on radon emanation (Tanner, 1980). Where data are adequate, exclusion isolines (figure 19) more accurately reflect the hazard potential than do the contoured soil-gas radon measurements (figure 18), and better validate the hazard-potential map (figure 30).

Hazard Potential and Indoor-Radon Levels

Geologic radon-hazard-potential maps cannot accurately characterize indoor-radon levels because indoor levels are also affected by non-geologic factors. A hazard-potential map does, however, provide an estimate of the underlying geologic basis for indoor-radon levels, which may be modified by non-geologic effects.

Of the 38 residential indoor-radon measurements in the central Sevier Valley (figure 21), only two were recorded in areas of low-hazard potential (table 7 and figure 30). The measurements, 5.3 and 5.4 pCi/L (196 and 200 Bq/m^3), were in nearby houses south of Venice. Although these measurements are greater than the range of probable indoor-radon concentrations in low-hazard-potential areas (table 6), the sample size is small, physically isolated, and not statistically representative of indoor-radon concentrations expected in a low-hazard-potential area. An additional 26 measurements were recorded in areas of moderate-hazard potential. The average of all measurements in areas of moderate-hazard potential is 3.7 pCi/L (137 Bq/m^3), within the range of probable indoor-radon concentrations in such hazard-potential areas. The average of 10 measurements in areas of high-hazard potential is 7.9 pCi/L (292 Bq/m^3), with 70 percent greater than 4 pCi/L (148 Bq/m^3). These levels are also consistent with probable indoor-radon levels.

Inconsistencies between the hazard assessment and indoor measurements arise because of the influence of unmeasured geologic and non-geologic factors, the presence of anomalies in

Table 7. *Residential indoor-radon concentrations in radon-hazard-potential categories for the central Sevier Valley. Average concentrations of the moderate and high categories are consistent with predicted values shown in table 6. Average concentration of the low category is inconsistent due to the inadequate sample size.*

	Hazard Category		
	Low	Moderate	High
Sample Size	2	26	10
Minimum	5.3	0.3	0.8
Average	5.4	3.7	7.9
Maximum	5.4	21.1	22.4
% ≥4 pCi/L	100	31	70
% of Total	5	68	26

measured factors not detected because of map scale, and the lack of a statistically valid sample of indoor measurements due to reliance on volunteers. In the absence of detailed indoor data, however, an assessment of the hazard potential based on easily obtainable geologic information is recommended. Indeed, one of the principal purposes of such a geologic assessment is to guide indoor testing to concentrate efforts on those areas for which geologic criteria indicate the greatest hazard potential. Once sufficient indoor data are obtained, average indoor-radon concentrations should better correlate with probable concentrations predicted by the geologic assessment, and the effect of other unmeasured factors should be relatively minor.

Cautions When Using This Report

Radon-hazard categories on the radon-hazard-potential map of the central Sevier Valley (figure 30) are relative and only comparable to other areas that have been mapped using identical classification criteria. This report should not be used to indicate absolute indoor-radon levels in specific buildings because a quantitative relationship between geologic factors and indoor-radon levels does not exist. Factors not considered can strongly affect indoor-radon levels.

All map boundaries between radon-hazard categories are approximate and gradational. Small, localized areas of higher or lower radon potential are likely to exist within any given map area, but their identification is precluded because of the effects of unconsidered factors and the limitations of map scale. The use of imported fill for foundation material can also affect the radon potential in small areas because the imported material may have different geologic characteristics than native soil.

Yokel and Tanner (1992) propose measurement methods and test procedures for the assessment of the radon source potential of individual building sites and fill materials. The methods and procedures are based on repeatable measurements of invariant soil properties, with corrections for typical prevailing environmental conditions. Protocols suggested by Yokel and Tanner (1992) may be unsuitable for some geologic materials, costly for certain types of development, and limited by equipment availability. However, appropriate use of these or similar protocols will provide information for sites at scales beyond the resolution of the radon-hazard-potential map of the central Sevier Valley.

CONCLUSIONS

The uranium content of soil and its bedrock source is the primary factor controlling indoor radon in the central Sevier Valley. Uranium and radon in soil gas exhibit a grossly linear relationship, and soil-gas radon is a precursor to indoor radon. However, numerous geologic and non-geologic factors also influence radon levels in both soil gas and indoors. Soil permeability and ground-water levels are two geologic factors which are readily characterized, and affect migration of radon in geologic materials. These factors, and uranium concentrations measured in a ground-based survey, were used in a numerical matrix to create a radon-hazard-potential map. The map confirms information from the NURE aerial radiometric survey that parts of the valley have high uranium concentrations and thus a potential for elevated indoor-radon levels, and adds considerable detail to the distribution of hazard areas. The map is also more detailed than the radon-hazard potential of the valley mapped in statewide compilations, and overcomes limitations of hazard mapping imposed by designating the hazard potential of areas defined by gross geologic or arbitrary political boundaries.

Areas of high-hazard potential are typically underlain by uraniferous Quaternary alluvial-fan deposits derived from Tertiary volcanic rocks. These deposits are common in the southern part of the valley between Monroe and Sevier, northward along the valley margins to Richfield on the west and Glenwood on the east, north and east of Vermillion, and on the eastern valley margin from Salina northward. Moderate soil permeability and deep ground water enhance radon emanation and migration in these areas.

Areas of moderate-hazard potential are typically underlain by Quaternary alluvial-fan and floodplain deposits with lower uranium contents. These deposits are derived from a mixture of sources composed predominantly of pre-volcanic sedimentary rocks, but with a significant volcanic component. They are common in the central part of the valley from Monroe northward, and along the central valley margins from Richfield to Vermillion on the west, and from Glenwood to Salina on the east. Permeability is moderate in these areas, but ground water tends to inhibit soil-gas radon migration during seasonal rises in ground-water tables.

Areas of low-hazard potential are typically underlain by Quaternary floodplain deposits with the lowest levels of uranium. These deposits are composed of sediment derived from both distant and local sources and transported to depositional areas by the Sevier River. They are restricted to the Sevier River floodplain between Annabella and Vermillion, and north of Aurora. The impermeable and poorly drained deposits are com-

mon in areas where ground water is forced upward by adjacent bedrock constrictions and discharged to the surface.

The relative hazard potential can be used to prioritize the dissemination of public information on the indoor-radon hazard, to indicate the urgency with which homeowners should test for the potential hazard in existing buildings, and to evaluate the need for radon-resistant new construction. The hazard-potential maps, however, are only reconnaissance tools. Detailed characterization and testing of specific sites are required to evaluate the influence of other factors, particularly the contribution of ^{220}Rn from the decay of ^{232}Th, and to overcome the limitation of map scale.

ACKNOWLEDGMENTS

This study was supported by a grant from the EPA, administered by the Utah Division of Radiation Control (UDRC), under the SIRG Program. John Hultquist, UDRC, was responsible for managing the SIRG Program in Utah and collecting indoor-radon measurements reported here. Many residents of the study areas provided consent for testing on their property; this study would not have been possible without them. This paper was reviewed by Gary Christenson, UGS, whom I thank for critical comments and helpful suggestions.

REFERENCES

Akerblom, Gustav, 1986, Investigation and mapping of radon risk areas: Lulea, Sweden, Swedish Geological Company, Report IRAP 86036, 15 p.

Anderson, R.E., and Barnhard, T.P., 1992, Neotectonic framework of the central Sevier Valley area, Utah, and its relationship to seismicity, *in* Gori, P.L., and Hays, W.W., editors, Assessment of regional earthquake hazards and risk along the Wasatch Front, Utah: U.S. Geological Survey Professional Paper 1500-F, 47 p.

Asher-Bolinder, Sigrid, Owen, D.E., and Schumann, R.R., 1990, Pedologic and climatic controls on Rn-222 concentrations in soil gas, Denver, Colorado: Geophysical Research Letters, v. 17, no. 6, p. 825-828.

Black, B.D., 1993, The radon-hazard-potential map of Utah: Utah Geological Survey Map 149, scale 1:1,000,000, 12 p. pamphlet.

Black, B.D., and Solomon, B.J., in preparation, Radon-hazard potential of the Weber River area, Tooele Valley, and southeast Cache Valley, Cache, Davis, Tooele, and Weber Counties, Utah: Utah Geological Survey Special Study.

Bromfield, C.S., Grauch, R.I., Otton, J.K., and Osmonson, L.M., 1982, National uranium resource evaluation, Richfield quadrangle, Utah: U.S. Geological Survey PGJ/F-044(82), 88 p.

Callaghan, Eugene, and Parker, R.L., 1961, Geologic map of the Monroe quadrangle, Utah: U.S. Geological Survey Geologic Quadrangle Map GQ-155, scale 1:62,500.

Carlisle, Donald, and Azzouz, Haydar, 1991, Geological parameters in radon risk assessment - a case history of deliberate exploration, *in* The 1991 International Symposium on Radon and Radon Reduction Technology, v. 5, preprints: Research Triangle Park, North Carolina, U.S. Environmental Protection Agency, Air and Energy Environmental Research Laboratory, p. IX-6.

Carmony, J.R., 1977, Stratigraphy and geochemistry of the Mount Belknap series, Tushar Mountains, Utah: University Park, Pennsylvania State University, M.S. thesis, 153 p.

Carpenter, C.H., and Young, R.A., 1963, Ground-water data, central Sevier Valley, parts of Sanpete, Sevier, and Piute Counties, Utah: U.S. Geological Survey Basic-Data Report No. 3, 34 p.

Conover, W.J., 1980, Practical nonparametric statistics, 2nd edition: New York, John Wiley & Sons, Inc., 493 p.

Cunningham, C.G., and Steven, T.A., 1979, Mount Belknap and Red Hills calderas and associated rocks, Marysvale volcanic field, west-central Utah: U.S. Geological Survey Bulletin 1468, 34 p.

Cunningham, C.G., Steven, T.A., Rowley, P.D., Glassgold, L.B., and Anderson, J.J., 1983, Geologic map of the Tushar Mountains and adjoining areas, Marysvale volcanic field, Utah: U.S. Geological Survey Miscellaneous Investigations Series Map I-1430-A, scale 1:50,000.

Dubiel, R.F., 1993, Preliminary geologic radon potential assessment of Utah, *in* Schumann, R.R., editor, Geologic radon potential of EPA Region 8: U.S. Geological Survey Open-File Report 93-292-H, p. 138-161.

Durrance, E.M., 1978, Radon in the stream waters of East Devon, *in* Edwards, R.A., editor, Proceedings of the 17th Ussher Society Conference: v. 4, pt. 2, p. 220-228.

Duval, J.S., 1983, Composite color images of aerial gamma-ray spectrometric data: Geophysics, v. 48, no. 6, p. 722-735.

—1991, Use of aerial gamma-ray data to estimate relative amounts of radon in soil gas, *in* Gundersen, L.C.S., and Wanty, R.B., editors, Field studies of radon in rocks, soil, and water: U.S. Geological Survey Bulletin 1971, p. 155-162.

Fleischer, R.L., Mogro-Compero, Antonio, and Turner, L.G., 1982, Radon levels in homes in the northeastern United States - energy-efficient homes, *in* Vohra, K.G., Mishra, U.C., Pillai, K.C., and Sadasivan, S., editors, Natural radiation environment: New York, John Wiley and Sons, p. 497-502.

Gilliland, W.N., 1963, Sanpete-Sevier Valley anticline of central Utah: Geological Society of America Bulletin, v. 74, no. 2, p. 115-124.

Gundersen, L.C.S., Gates, A.E., Schultz, A.P., Schumann, R.R., Speer, J.A., and Stanton, M.R., 1993, An investigation of the geology and geochemistry of radon in sheared and fractured rocks, *in* Rose, S.L., editor, FY-1992 radon research program: U.S. Department of Energy, Office of Energy Research and Office of Health and Environmental Research, DOE/ER-0588, p. 57-61.

Hecker, Suzanne, Harty, K.M., and Christenson, G.E., 1988, Shallow ground water and related hazards in Utah: Utah Geological and Mineral Survey Map 110, scale 1:750,000, 17 p. pamphlet.

Hesselbom, A., 1985, Radon in soil gas - a study of methods and instruments for determining radon concentrations in the ground: Sveriges Geologiska Undersokning (Swedish Geological Survey) Ser. C-803 (in English).

Holford, D.J., Schery, S.D., Wilson, J.L., and Phillips, F.M., 1993, Modeling radon transport in dry, cracked soil: Journal of Geophysical Research, v. 98, no. B1, p. 567-580.

Kraner, H.W., Schroeder, G.L., and Evans, R.D., 1964, Measurements of the effects of atmospheric variables on radon-222 flux and soil-gas concentration, *in* Adams, J.A.S., and Lowder, W.M., editors, The natural radiation environment: Chicago, University of Chicago Press, p. 191-215.

Lautenschlager, H.K., 1952, The geology of the central part of the Pahvant Range, Utah: Columbus, Ohio State University, Ph.D. thesis, 188 p., scale 1:31,680.

Lupe, R.D., Campbell, J.A., Franczyk, K.J., Luft, S.J., Peterson, Fred, and Robinson, Keith, 1982, National uranium resource evaluation, Salina quadrangle, Utah: U.S. Geological Survey PGJ/F-053(82), 83 p.

Mabey, D.R., and Budding, K.E., 1987, High-temperature geothermal resources of Utah: Utah Geological and Mineral Survey Bulletin 123, 64 p.

McCammon, R.B., 1980, The statistical treatment of geochemical data, *in* Levinson, A.A., editor, Introduction to exploration geochemistry, 2nd edition: Toronto, Applied Publishing Ltd., p. 835-843.

McLemore, V.T., Hawley, J.W., and Manchego, R.A., 1991, Geologic evaluation of radon availability in New Mexico - a progress report, *in* The 1991 International Symposium on Radon and Radon Reduction Technology, v. 5, preprints: Research Triangle Park, North Carolina, U.S. Environmental Protection Agency, Air and Energy Environmental Research Laboratory, p. IXP-1.

Meussig, K.W., 1988, Correlation of airborne radiometric data and geologic sources with elevated indoor radon in New Jersey, *in* The 1988 Symposium on Radon and Radon Reduction Technology, Denver, Colorado, preprints: Research Triangle Park, North Carolina, U.S. Environmental Protection Agency, Air and Energy Environmental Research Laboratory, EPA/600/9-89/006a, v. 1, p. V-1.

Morris, H.T., 1987, Preliminary geologic map of the Delta 2° quadran-

gle, Tooele, Juab, Millard, and Utah Counties: U.S. Geological Survey Open-File Report 87-185, 22 p., scale 1:250,000.

National Council on Radiation Protection and Measurements, 1984, Evaluation of occupational and environmental exposures to radon and radon daughters in the United States: Bethesda, Maryland, National Council on Radiation Protection and Measurements Report 78, 204 p.

Nielson, D.L., 1978, Radon emanometry as a geothermal exploration technique; theory and an example from Roosevelt Hot Springs KGRA, Utah: Salt Lake City, University of Utah Research Institute, Earth Science Laboratory, IDO/78-1701.b.1.1.2, ESL-14, 30 p.

Nielson, D.L., Linpei, Cui, and Ward, S.H., 1991, Gamma-ray spectrometry and radon emanometry in environmental geophysics, *in* Ward, S.H., editor, Geotechnical and environmental geophysics, v. 1, - review and tutorial: Tulsa, Oklahoma, Society of Exploration Geophysicists, p. 219-250.

Peake, R.T., and Schumann, R.R., 1991, Regional radon characteristics, *in* Gundersen, L.C.S., and Wanty, R.B., editors, Field studies of radon in rocks, soil, and water: U.S. Geological Survey Bulletin 1971, p. 163-175.

Reimer, G.M., and Bowles, C.G., 1979, Soil-gas helium concentrations in the vicinity of a uranium deposit, Red Desert, Wyoming: U.S. Geological Survey Open-File Report 79-975, 10 p.

Reimer, G.M., and Gundersen, L.C.S., 1989, A direct correlation among indoor Rn, soil gas Rn, and geology in the Reading Prong near Boyertown, Pennsylvania: Health Physics, v. 57, no. 1, p. 155-160.

Robinson, T.W., 1958, Phreatophytes: U.S. Geological Survey Water-Supply Paper 1423, 84 p.

Rogers, A.S., 1958, Physical behavior and geological control of radon in mountain streams: U.S. Geological Survey Bulletin 1952E, p. 187-211.

Rogers, J.J.W., 1964, Statistical tests of the homogeneity of the radioactive components of granitic rocks, *in* Makofske, W.J., and Edelstein, M.R., editors, Radon and the environment: Park Ridge, New Jersey, Noyes Publications, p. 51-62.

Rogers, V.C., and Nielson, K.K., 1990, Benchmark and application of the RAETRAD model, *in* The 1990 International Symposium on Radon and Radon Reduction Technology, Atlanta, Georgia, preprints: Research Triangle Park, North Carolina, U.S. Environmental Protection Agency, Air and Energy Environmental Research Laboratory, EPA/600/9-90/005c, v. 3, p. VI-1.

Rowley, P.D., Cunningham, C.G., and Kaplan, A.M., 1981, Geologic map of the Monroe SE quadrangle, Sevier and Piute Counties, Utah: U.S. Geological Survey Miscellaneous Field Studies Map MF-1331, scale 1:24,000.

Rowley, P.D., Cunningham, C.G., Steven, T.A., Mehnart, H.H., and Naeser, C.W., 1988, Geologic map of the Antelope Range quadrangle, Sevier and Piute Counties, Utah: Utah Geological and Mineral Survey Map 106, scale 1:24,000, 14 p.

Rowley, P.D., Steven, T.A., and Kaplan, A.M., 1981, Geologic map of the Monroe NE quadrangle, Sevier County, Utah: U.S. Geological Survey Miscellaneous Field Studies Map MF-1330, scale 1:24,000.

Samet, J.M., 1989, Radon exposure and lung cancer risk, *in* The 1988 Symposium on Radon and Radon Reduction Technology, Denver, Colorado, preprints: Research Triangle Park, North Carolina, U.S. Environmental Protection Agency, Air and Energy Environmental Research Laboratory, EPA/600/9-89/006a, v. I, p. II-1.

Schery, S.D., and Siegel, D., 1986, The role of channels in the transport of radon from soil: Journal of Geophysical Research, v. 91, p. 12,266-12,374.

Schery, S.D., Gaeddert, D.H., and Wilkening, M.H., 1982, Transport of radon from fractured rock: Journal of Geophysical Research, v. 87, p. 2969-2976.

Schumann, R.R., Owen, D.E., and Asher-Bolinder, Sigrid, 1992, Effects of weather and soil characterization on temporal variations in soil-gas radon concentrations, *in* Gates, A.E., and Gundersen, L.C.S., editors, Geologic controls on radon: Geological Society of America Special Paper 271, p. 65-72.

Sextro, Richard, 1988, Radon in dwellings, *in* Makofske, W.J., and Edelstein, M.R., editors, Radon and the environment: Park Ridge, New Jersey, Noyes Publications, p. 71-82.

Sinclair, A.J., 1976, Application of probability graphs in mineral exploration: The Association of Exploration Geochemists, Special Volume 4, 95 p.

—1986, Statistical interpretation of soil geochemical data, *in* Berger, B.R., and Bethke, P.M., editors, Exploration geochemistry - design and interpretation of soil surveys: Reviews in Economic Geology, v. 3, p. 97-115.

Solomon, B.J., 1992, Environmental geophysical survey of radon-hazard areas in the southern St. George basin, Washington County, Utah, *in* Harty, K.M., editor, Engineering and environmental geology of southwestern Utah: Utah Geological Association Publication 21, p. 173-191.

Solomon, B.J., Black, B.D., Finerfrock, D.L., and Hultquist, John, 1993, Geologic mapping of radon-hazard potential in Utah, *in* The 1993 International Radon Conference, Denver, Colorado, preprints: Denver, American Association of Radon Scientists and Technologists, p. IVP 14-IVP 28.

Solomon, B.J., Black, B.D., Nielson, D.L., Finerfrock, D.L., Hultquist, J.D., and Cui, Linpei, 1994, Radon-hazard-potential areas in Sandy, Salt Lake County, and Provo, Utah County, Utah: Utah Geological Survey Special Study 85, 49 p.

Sprinkel, D.A., and Solomon, B.J., 1990, Radon hazards in Utah: Utah Geological and Mineral Survey Circular 81, 24 p.

Steven, T.A., 1979, Geologic map of the Monroe NW quadrangle, west-central Utah: U.S. Geological Survey Miscellaneous Field Studies Map MF-1107, scale 1:24,000.

Steven, T.A., and Cunningham, C.G., 1979, Geologic map of the Sevier SE quadrangle, west-central Utah: U.S. Geological Survey Miscellaneous Field Studies Map MF-1109, scale 1:24,000.

Steven, T.A., Morris, H.T., and Rowley, P.D., 1990, Geologic map of the Richfield $1^{\circ} \times 2^{\circ}$ quadrangle, west-central Utah: U.S. Geological Survey Miscellaneous Investigations Map I-1091, scale 1:250,000.

Stoker, A.K., and Kruger, P., 1975, Radon in geothermal reservoirs: San Francisco, Second United Nations Symposium on the Development and Use of Geothermal Resources, p. 1797-1803.

Stokes, W.G., 1977, Physiographic subdivisions of Utah: Utah Geological and Mineral Survey Map 43, scale 1:2,400,000.

Stranden, Erling, 1984, Thoron (^{220}Rn) daughter to radon (^{222}Rn) daughter ratios in thorium-rich areas: Health Physics, v. 47, no. 5, p. 784-785.

Tanner, A.B., 1980, Radon migration in the ground - a supplementary review, *in* Gesell, T.F., and Lowder, W.M., editors, Natural Radiation Environment III, Symposium Proceedings: Houston, U.S. Department of Energy Report CONF-780422, v. 1, National Technical Information Service, p. 5-56.

—1986, Indoor radon and its sources in the ground: U.S. Geological Survey Open-File Report 86-222, 5 p.

—1989, The source of radon in houses, *in* Harley, N.H., editor, Radon,

Proceedings of the Twenty-Fourth Annual Meeting of the National Council on Radiation Protection and Measurements, Washington, D.C., March 30-31, 1988: Bethesda, Maryland, National Council on Radiation Protection and Measurements, Proceedings Series No. 10, p. 159-169.

—1991a, Error in measuring radon in soil gas by means of passive detectors: Nuclear Geophysics, v. 5, p. 25-30.

—1991b, Methods of characterization of ground for assessment of indoor radon potential at a site, *in* Gundersen, L.C.S., and Wanty, R.B., editors, Field studies of radon in rocks, soils, and water: U.S. Geological Survey Bulletin 1971, p. 1-18.

U.S. Environmental Protection Agency, 1989a, Guidance for the State Indoor Radon Grants Program, Section 306, Indoor Radon Abatement Act: U.S. Environmental Protection Agency, Office of Radiation Programs, 47 p.

—1989b, Radon measurement in schools, an interim report: U.S. Environmental Protection Agency Report EPA-520/1-89-010, 17 p.

—1992, A citizen's guide to radon (second edition) - the guide to protecting yourself and your family from radon: U.S. Environmental Protection Agency, U.S. Department of Health and Human Services, and U.S. Public Health Service, 402-K92-001, 15 p.

—1993, EPA's map of radon zones - Utah: U.S. Environmental Protection Agency, Office of Radiation and Indoor Air, Radon Division, 402-R-93-064, 5 chapters, individually paginated.

Utah Office of Planning and Budget, 1991, 1990 census brief - cities and counties of Utah: Salt Lake City, Utah Office of Planning and Budget, Demographic and Economic Analysis Section, 37 p.

Williams, P.L., and Hackman, R.J., 1971, Geology, structure, and uranium deposits of the Salina quadrangle, Utah: U.S. Geological Survey Miscellaneous Geologic Investigations Map I-591, scale 1:250,000.

Willis, G.C., 1986, Geologic map of the Salina quadrangle, Sevier County, Utah: Utah Geological and Mineral Survey Map 83, scale 1:24,000, 20 p. pamphlet.

—1988, Geologic map of the Aurora quadrangle, Sevier County, Utah: Utah Geological and Mineral Survey Map 112, scale 1:24,000, 21 p. pamphlet.

—1991, Geologic map of the Redmond Canyon quadrangle, Sanpete and Sevier Counties, Utah: Utah Geological Survey Map 138, scale 1:24,000, 17 p. pamphlet.

—1994, Interim geologic map of the Richfield quadrangle, Sevier County, Utah: Utah Geological Survey Open-File Report 309, scale 1:24,000, 73 p. pamphlet.

Wilson, Carole, 1987, Radon--geological aspects of an environmental problem: The Amateur Geologist, v. 11, no. 2, p. 17-33.

Wilson, Le Moyne, Jennings, D.S., Rickenbach, R.G., Gourley, Rex, Nielson, J.E., Frost, R.L., Adair, J.S., and Rabe, F.S., 1958, Soil survey of Richfield area, Utah: U.S. Department of Agriculture, Soil Conservation Service, in cooperation with Utah Agricultural Experiment Station, Series 1944, no. 9, 93 p.

Witkind, I.J., Weiss, M.P., and Brown, T.L., 1987, Geologic map of the Manti 30′ x 60′ quadrangle, Carbon, Emery, Juab, Sanpete, and Sevier Counties, Utah: U.S. Geological Survey Miscellaneous Investigations Series Map I-1631, scale 1:100,000.

Yokel, F.Y., and Tanner, A.B., 1992, Site exploration for radon source potential: Gaithersburg, Maryland, Building and Fire Research Laboratory, National Institute of Standards and Technology, NISTIR 5135, 61 p.

Young, R.A., and Carpenter, C.H., 1965, Ground-water conditions and storage in the central Sevier Valley, Utah: U.S. Geological Survey Water-Supply Paper 1787, 95 p.

APPENDIX

Table A-1. *Radiometric data from the central Sevier Valley, exclusive of indoor-radon measurements. K - potassium-40; eU - equivalent uranium-238; eTh - equivalent thorium-232; eU/eTh - ratio of eU and eTh; Rn - radon-222; ND - no data, samples were not collected from these sites.*

Sample Number	Location			Total Gamma (ppm)	K (%)	eU (ppm)	eTh (ppm)	eU/eTh	Soil-Gas Rn (pCi/L)
	Township	Range	1/4 Section						
R-001	25S	3W	SE15	15.2	2.4	3.5	9.3	0.38	389.36
R-002	25S	3W	SW16	21.6	2.9	5.0	17.1	0.29	622.52
R-003	25S	3W	NW17	27.2	2.9	7.2	24.9	0.29	1,107.84
R-004	25S	3W	NW18	21.4	2.7	5.1	19.4	0.26	668.89
R-005	25S	4W	NW13	20.4	3.1	3.8	14.7	0.26	146.19
R-006	26S	4W	NE24	27.3	3.4	7.2	20.8	0.35	ND
R-007	26S	3W	NE19	34.3	4.0	8.6	32.9	0.26	ND
R-008	26S	3W	SE20	29.4	3.7	5.7	25.2	0.23	ND
R-009	26S	3W	SE21	21.4	3.0	4.9	15.7	0.31	ND
R-010	25S	3W	NE22	23.9	3.1	4.6	19.3	0.24	ND
R-011	25S	4W	NE14	16.0	2.4	3.6	11.6	0.31	419.32
R-012	25S	4W	NE15	20.7	2.6	5.9	16.9	0.35	ND
R-013	25S	4W	NE16	18.3	2.5	4.1	15.6	0.26	ND
R-014	25S	4W	SE2	16.2	2.4	1.9	14.7	0.13	128.50
R-015	25S	4W	NE1	16.8	2.4	4.4	13.7	0.32	110.00
R-016	25S	4W	SE21	23.8	3.2	5.0	19.8	0.25	ND
R-017	25S	4W	SE22	26.9	3.5	5.4	24.8	0.22	349.23
R-018	25S	4W	NW23	17.3	2.2	4.0	14.2	0.28	ND
R-019	25S	4W	SE11	16.0	2.2	3.5	14.2	0.25	368.46
R-020	25S	4W	NE12	23.0	2.9	5.0	19.9	0.25	ND
R-021	25S	3W	SE6	13.2	1.7	2.5	11.2	0.22	234.15
R-022	25S	4W	NE27	18.8	2.6	3.5	15.0	0.23	276.75
R-023	25S	4W	NW28	25.8	3.1	6.2	23.5	0.26	ND
R-024	25S	4W	SE29	24.6	2.9	6.3	20.4	0.31	ND
R-025	25S	4W	NE30	27.8	3.2	5.7	25.3	0.23	210.55
R-026	25S	4W	SE31	37.5	4.0	8.7	36.1	0.24	ND
R-027	25S	4W	SE32	26.3	3.6	4.5	26.0	0.17	ND
R-028	25S	4W	NW33	25.1	3.1	6.2	21.1	0.29	625.13
R-029	25S	3W	SE7	21.5	2.7	4.6	18.7	0.25	200.58
R-030	25S	3W	NE8	27.9	3.2	6.6	27.2	0.24	ND
R-031	25S	3W	SW2	22.5	3.1	5.8	17.1	0.34	275.22
R-032	25S	3W	NW3	15.5	2.3	3.5	12.3	0.28	206.13
R-033	25S	3W	NW4	17.0	1.9	4.4	15.3	0.29	ND
R-034	25S	3W	SW5	15.7	1.9	3.9	12.4	0.31	ND

***Table A-1** (continued)*

R-035	24S	4W	SE25	32.4	4.0	9.5	27.7	0.34	442.64
R-036	24S	4W	NW36	16.7	2.4	4.1	12.8	0.32	ND
R-037	25S	3W	NW9	21.5	3.0	3.8	19.3	0.20	548.80
R-038	25S	3W	SW11	25.7	2.2	14.1	12.0	1.18	378.61
R-039	25S	3W	NW10	16.1	2.4	4.4	10.1	0.44	ND
R-040	24S	3W	SE31	27.7	3.5	6.6	21.0	0.31	ND
R-041	24S	3W	SW30	26.5	3.8	5.6	22.9	0.24	ND
R-042	24S	3W	SE29	17.7	2.4	4.1	13.1	0.31	126.89
R-043	24S	3W	SE28	15.5	2.0	3.5	11.2	0.31	209.70
R-044	24S	3W	NE27	11.5	1.7	3.2	7.4	0.43	735.03
R-045	24S	3W	SW26	16.3	2.5	3.4	10.1	0.34	299.89
R-046	24S	3W	NE22	19.6	2.6	3.6	18.6	0.19	240.51
R-047	24S	3W	NE33	16.6	2.3	2.6	16.0	0.16	ND
R-048	24S	3W	NE34	13.3	1.9	3.3	8.9	0.37	ND
R-049	24S	3W	SW35	21.7	3.2	4.9	17.3	0.28	ND
R-050	24S	3W	NE36	27.8	3.4	6.0	24.3	0.25	ND
R-051	24S	3W	SE16	11.4	1.5	3.7	8.0	0.46	ND
R-052	24S	3W	SW15	13.9	1.7	4.2	8.9	0.47	195.17
R-053	24S	3W	SW14	12.5	1.7	4.4	9.1	0.48	197.97
R-054	24S	3W	NW13	13.4	2.0	2.8	8.4	0.33	38.94
R-055	24S	3W	SE25	26.5	3.1	7.1	22.3	0.32	ND
R-056	24S	3W	SE24	20.7	2.7	5.8	16.4	0.35	477.94
R-057	24S	3W	SE20	18.1	2.7	3.9	14.6	0.27	ND
R-058	24S	3W	SW21	10.9	1.3	3.3	8.0	0.41	145.74
R-059	24S	3W	SE22	11.5	1.7	2.4	6.5	0.37	ND
R-060	24S	3W	NW23	12.1	1.9	3.2	9.4	0.34	ND
R-061	24S	3W	NE3	18.0	2.4	3.9	15.7	0.25	ND
R-062	24S	3W	SW2	12.5	1.8	3.1	8.8	0.35	165.39
R-063	24S	3W	SE9	13.2	1.8	4.8	7.0	0.69	138.07
R-064	24S	2W	NW18	11.7	1.6	3.1	6.8	0.46	149.15
R-065	24S	2W	SW17	15.6	2.3	4.0	11.7	0.34	150.85
R-066	24S	2W	NW16	21.0	2.9	4.5	16.2	0.28	ND
R-067	24S	2W	SE20	14.2	2.4	3.2	8.7	0.37	ND
R-068	24S	2W	NE19	15.6	2.3	4.3	9.9	0.43	ND
R-069	24S	3W	NW10	10.0	1.5	2.1	8.3	0.25	342.58
R-070	24S	3W	SW11	11.5	1.5	3.4	8.0	0.43	ND

***Table A-1** (continued)*

R-071	24S	3W	NW1	11.2	1.5	2.8	8.8	0.32	211.09
R-072	24S	2W	NW6	9.4	1.3	2.1	6.6	0.32	630.13
R-073	24S	2W	NW5	10.0	1.4	1.5	8.3	0.18	699.16
R-074	24S	2W	SW4	19.9	2.9	4.7	13.8	0.34	ND
R-075	24S	2W	NE3	14.0	1.9	3.9	10.7	0.36	ND
R-076	24S	2W	SE10	16.8	2.4	4.1	13.2	0.31	ND
R-077	24S	2W	SW9	26.3	3.5	5.8	20.5	0.28	ND
R-078	24S	2W	SE8	13.5	1.7	3.2	8.8	0.36	ND
R-079	24S	2W	NE7	14.8	2.0	4.3	12.0	0.36	432.20
R-080	24S	3W	NW12	11.4	1.6	1.9	9.0	0.21	285.06
R-081	23S	3W	SW26	11.6	1.7	2.7	8.8	0.31	ND
R-082	23S	3W	NW25	7.4	0.8	1.9	5.1	0.37	102.54
R-083	23S	2W	NW30	6.7	0.9	2.1	4.2	0.50	319.54
R-084	23S	2W	NE29	7.2	1.0	1.7	4.6	0.37	411.08
R-085	24S	2W	SW1	27.7	3.4	6.0	24.1	0.25	376.20
R-086	23S	2W	NE33	27.8	3.8	6.2	20.4	0.30	ND
R-087	23S	2W	SE32	10.5	1.4	1.9	10.0	0.19	150.76
R-088	23S	2W	SE32	11.2	1.7	3.0	6.5	0.46	ND
R-089	23S	3W	SW36	9.7	1.3	2.5	6.7	0.37	ND
R-090	23S	3W	NW35	12.7	1.7	4.0	8.8	0.45	ND
R-091	23S	2W	SW28	8.8	1.1	3.0	6.2	0.48	97.34
R-092	23S	2W	SE27	12.1	1.6	3.1	9.7	0.32	0.00
R-093	23S	2W	NE26	13.4	2.1	2.5	9.6	0.26	227.29
R-094	23S	2W	NE25	15.4	2.4	2.1	12.7	0.17	233.12
R-095	23S	1W	NW30	39.9	4.3	11.5	31.9	0.36	276.42
R-096	23S	2W	SE24	13.5	2.2	2.6	9.2	0.28	ND
R-097	23S	2W	SW36	15.5	2.4	3.4	11.4	0.30	ND
R-098	23S	2W	NE35	21.7	2.9	3.6	21.0	0.17	ND
R-099	23S	2W	NW34	13.0	1.7	3.8	11.2	0.34	ND
R-100	23S	2W	SW23	10.8	1.8	2.2	6.1	0.36	ND
R-101	23S	2W	NW15	12.9	2.1	3.1	10.1	0.31	565.78
R-102	23S	2W	NW16	8.7	1.2	2.7	5.8	0.47	192.80
R-103	23S	2W	SE17	6.8	0.9	1.9	3.9	0.49	83.09
R-104	23S	2W	NE18	7.0	0.9	2.0	5.0	0.40	42.39
R-105	23S	2W	SE14	11.9	2.2	1.8	7.6	0.24	52.21
R-106	23S	2W	SW22	8.3	1.0	1.7	8.5	0.20	ND

Table A-1 (continued)

R-107	23S	2W	NW21	8.1	1.2	1.8	6.6	0.27	ND
R-108	23S	2W	SE20	7.1	1.0	1.1	5.7	0.19	ND
R-109	23S	2W	NE19	7.7	1.2	1.7	4.8	0.35	ND
R-110	23S	3W	NW24	6.3	0.8	2.0	4.7	0.43	ND
R-111	23S	2W	NW3	5.6	0.5	2.0	3.6	0.56	156.73
R-112	23S	2W	SE4	4.4	0.7	0.9	3.2	0.28	357.42
R-113	23S	2W	SW2	6.9	0.9	2.3	5.0	0.46	83.06
R-114	23S	1W	SW18	12.3	2.1	2.0	9.6	0.21	92.39
R-115	23S	2W	SE13	21.4	3.2	3.7	17.7	0.21	166.46
R-116	23S	1W	NW8	9.3	1.6	1.0	7.0	0.14	ND
R-117	23S	1W	NW7	15.9	3.0	2.0	9.7	0.21	ND
R-118	23S	2W	SE12	12.2	2.0	2.6	8.1	0.32	ND
R-119	23S	2W	NW11	6.3	0.9	1.8	3.9	0.46	ND
R-120	23S	3W	NE23	6.5	0.8	2.3	5.2	0.44	ND
R-121	22S	2W	SE28	7.7	0.9	2.9	6.5	0.45	141.00
R-122	22S	2W	SW27	5.7	0.7	1.7	4.7	0.36	ND
R-123	22S	2W	NE33	5.0	0.5	2.4	3.5	0.69	ND
R-124	23S	1W	SW5	10.7	2.2	2.3	5.5	0.42	53.36
R-125	23S	1W	SE6	11.1	1.9	2.3	5.4	0.43	ND
R-126	23S	2W	SE1	11.7	2.1	2.0	8.1	0.25	94.86
R-127	23S	2W	NE7	5.3	0.5	1.8	3.7	0.49	ND
R-128	23S	2W	NW8	4.8	0.4	2.5	2.4	1.04	ND
R-129	23S	2W	NW9	6.4	0.8	2.0	4.0	0.50	538.23
R-130	23S	2W	NW10	7.3	1.1	1.8	5.9	0.31	279.16
R-131	22S	2W	NE26	7.1	0.8	2.6	6.6	0.39	ND
R-132	22S	2W	SW25	5.3	0.5	2.0	3.7	0.54	ND
R-133	22S	1W	SW31	13.9	2.4	2.9	8.2	0.35	45.09
R-134	22S	1W	SE30	25.7	3.7	5.5	20.1	0.27	ND
R-135	22S	1W	SE32	7.8	1.6	1.9	3.7	0.51	84.67
R-136	22S	1W	SE29	9.9	1.7	2.5	4.0	0.63	110.52
R-137	22S	1W	NW28	9.9	2.0	1.8	4.4	0.41	ND
R-138	22S	2W	SE34	4.1	0.3	1.7	3.1	0.55	ND
R-139	22S	2W	NW35	5.1	0.5	1.8	3.9	0.46	33.77
R-140	22S	2W	SW36	6.4	0.9	1.5	4.5	0.33	106.64
R-141	22S	1W	NW17	9.0	1.1	3.7	5.6	0.66	119.27
R-142	22S	1W	NW14	9.9	1.7	2.6	5.2	0.50	64.15

Table A-1 *(continued)*

R-143	22S	1W	SE16	10.0	1.7	2.0	6.8	0.29	89.88
R-144	22S	1W	NW33	7.8	1.5	1.2	4.6	0.26	ND
R-145	22S	1W	SW18	7.1	0.9	2.2	4.8	0.46	ND
R-146	22S	2W	NW13	7.6	1.0	2.0	5.5	0.36	128.09
R-147	22S	1W	NW3	12.0	1.7	2.7	8.7	0.31	112.38
R-148	22S	1W	SE4	10.7	1.4	3.3	7.0	0.47	147.79
R-149	22S	1W	NE5	12.1	1.9	2.8	7.8	0.36	ND
R-150	22S	1W	SE6	7.8	0.9	3.1	3.8	0.82	ND
R-151	22S	2W	SW1	11.6	1.1	5.1	7.8	0.65	ND
R-152	22S	2W	NW24	6.7	0.8	2.4	5.6	0.43	ND
R-153	22S	2W	NE14	8.2	0.9	3.9	4.2	0.93	ND
R-154	22S	2W	SW23	6.2	0.7	1.9	5.6	0.34	ND
R-155	22S	2W	NE22	5.4	0.5	2.0	4.6	0.43	ND
R-156	22S	1W	NE20	31.0	4.0	9.3	23.5	0.40	ND
R-157	22S	1W	NW20	20.4	2.8	5.2	16.1	0.32	324.21
R-158	21S	1W	SE27	9.0	1.2	3.2	6.8	0.47	62.17
R-159	21S	1W	NE26	9.1	1.2	2.5	6.2	0.40	287.54
R-160	21S	1W	NE25	11.0	1.3	3.8	9.0	0.42	102.30
R-161	21S	1E	NW30	43.5	4.4	11.3	41.9	0.27	265.50
R-162	22S	1W	NW1	13.1	1.9	2.9	9.9	0.29	130.84
R-163	22S	1W	NE2	10.9	1.8	3.0	5.7	0.53	69.66
R-164	22S	1W	NW10	13.4	1.8	3.4	9.5	0.36	ND
R-165	22S	1W	NW9	15.5	2.0	4.3	11.9	0.36	ND
R-166	22S	1W	NW8	10.0	1.2	3.6	6.0	0.60	ND
R-167	22S	1W	NW7	7.0	1.1	2.0	5.6	0.36	ND
R-168	22S	2W	SW12	6.9	0.9	1.8	4.4	0.41	ND
R-169	21S	1W	NW24	11.0	1.4	2.7	7.2	0.38	173.94
R-170	21S	1E	NW19	10.9	1.5	3.7	7.0	0.53	189.29
R-171	21S	1W	NE36	11.6	1.7	3.5	8.9	0.39	124.62
R-172	21S	1W	NE30	5.4	0.4	3.2	3.3	0.97	99.98
R-173	21S	1W	SW29	11.5	1.7	2.4	8.8	0.27	97.50
R-174	21S	1W	SW28	8.8	1.2	2.9	6.0	0.48	193.37
R-175	21S	1W	SE31	11.3	1.1	4.6	8.1	0.57	ND
R-176	21S	1W	SW32	10.0	1.4	2.7	6.2	0.44	ND
R-177	21S	1W	SE33	9.6	1.1	2.6	8.1	0.32	ND
R-178	21S	1W	NW34	9.4	1.4	2.0	7.7	0.26	ND

Table A-1 *(continued)*

R-179	21S	1W	NE35	16.4	2.5	4.2	9.3	0.45	ND
R-180	21S	1E	SE18	8.5	1.0	3.1	5.6	0.55	ND
R-181	21S	1E	NE17	21.5	2.4	6.1	15.7	0.39	224.87
R-182	21S	1W	SW13	12.0	1.7	2.9	8.9	0.33	197.26
R-183	21S	1W	SW14	14.8	1.7	4.7	11.8	0.40	770.44
R-184	21S	1W	NE15	9.5	1.0	3.0	8.1	0.37	107.17
R-185	21S	1W	SW16	7.9	0.8	2.7	6.1	0.44	163.86
R-186	21S	1W	NE17	5.8	0.4	3.2	3.5	0.91	ND
R-187	21S	1W	SE20	5.8	0.5	3.0	3.8	0.79	ND
R-188	21S	1W	SW21	7.7	0.8	2.9	4.9	0.59	ND
R-189	21S	1W	NW22	9.1	1.2	2.7	6.5	0.42	ND
R-190	21S	1W	SE23	9.4	1.4	2.3	5.9	0.39	ND
R-191	21S	1E	NW5	10.0	1.0	3.8	7.3	0.52	105.58
R-192	21S	1E	SE6	10.9	1.3	2.8	10.1	0.28	76.06
R-193	21S	1W	SW1	14.6	2.1	4.4	11.6	0.38	143.50
R-194	21S	1W	SW2	16.0	2.1	4.2	13.6	0.31	126.71
R-195	21S	1W	SE3	9.4	1.2	2.0	7.8	0.26	53.35
R-196	21S	1W	NW9	6.7	0.6	2.2	5.4	0.41	ND
R-197	21S	1W	SW10	7.3	0.8	2.7	4.5	0.60	ND
R-198	21S	1W	NW11	11.4	1.6	2.9	8.4	0.35	ND
R-199	21S	1W	SE12	18.1	2.2	3.7	17.4	0.21	ND
R-200	21S	1E	NW7	13.8	2.4	1.8	10.3	0.17	ND
R-201	22S	1W	NW11	22.0	3.0	4.2	21.5	0.20	ND
R-202	22S	1W	NW15	10.8	1.5	2.3	9.6	0.24	ND

Table A-2. *Residential indoor-radon measurements from the central Sevier Valley, listed in descending order of indoor-radon levels by community and zip code. A hazard-potential-category for each residential location was determined from the hazard-potential map (figure 30). Detector 35181, Joseph, was not returned (NR). Rn - radon-222.*

Detector Number	Location			Indoor Rn (pCi/L)	Hazard Category
	Township	Range	1/4 Section		
Elsinore - 84704					
35136	24S	3W	NW28	3.5	high
Joseph - 84739					
483349	25S	4W	SW2	1.7	moderate
35181	25S	4W	SE22	NR	high
Monroe - 84754					
483705	25S	3W	SE16	22.4	high
483490	25S	3W	NE16	21.1	moderate
35009	25S	3W	SW15	12.7	high
483823	25S	3W	SE15	10.0	high
35444	25S	3W	SE9	9.9	moderate
35140	25S	3W	NE15	7.6	high
34993	25S	3W	NE22	6.5	high
35263	25S	3W	SW10	4.9	moderate
35055	25S	3W	SW10	3.4	moderate
483498	25S	3W	SW10	2.7	moderate
35057	25S	3W	SW10	2.2	moderate
634623	25S	3W	SE15	1.7	high
Richfield - 84701					
35076	23S	3W	SW25	6.8	moderate
35154	23S	3W	NE35	6.4	moderate
483256	23S	3W	SE35	4.4	moderate
35095	23S	3W	SE26	4.3	moderate
483183	23S	3W	NE26	4.0	moderate
34972	23S	3W	NE35	3.3	moderate
35264	23S	3W	SE23	2.1	moderate
483292	23S	3W	SE35	2.1	moderate
483833	23S	3W	NE35	2.1	moderate
35432	23S	3W	SW35	2.0	moderate
34985	23S	3W	NW35	1.7	moderate
35441	23S	3W	NW25	1.7	moderate
35237	23S	3W	NE35	1.5	moderate
35435	23S	3W	NW25	1.4	moderate
483496	23S	3W	SW25	1.3	moderate

***Table A-2** (continued)*

483811	23S	2W	NW19	1.2	moderate
35217	23S	3W	NW25	0.3	moderate
Salina - 84654					
35161	21S	1W	NE25	0.8	moderate
Sevier - 84766					
35078	25S	4W	NE32	7.2	high
35062	25S	4W	SW28	6.6	high
483257	25S	4W	NE28	0.8	high
Sigurd - 84656					
35066	23S	2W	NE1	2.6	moderate
Venice - 84701					
34975	23S	2W	SE15	5.4	low
483494	23S	2W	SW15	5.3	low

Table A-3. *School indoor-radon measurements from the central Sevier Valley. Rn - radon-222.*

Detector Number	Room	Indoor Rn (pCi/L)	Comments
South Sevier Middle School			
20911	Media Room	2.8	---
20983	Media Room	2.1	Tunnel Area
20981	Band Room	1.4	---
20905	Auditorium	0.7	---
20985	Office	0.6	Deer Horn
20994	Cafeteria	0.6	---
20995	Main Hall	0.6	Main Hall North
20986	Shop Room	0.5	---
20990	South Hall	0.1	---
20957	Gym - West End	---	Void
20964	Boiler Room	---	Void
20991	Home Economics	---	Detector Missing
20997	Gym - East End	---	Detector Missing
South Sevier High School			
21063	Kitchen	5.1	Store Room
21066	Gym	3.7	Red Panels - SW
21061	Gym	3.6	Red Panels - NE
21067	Media Center	3.5	Basket - South
20993	Office	2.7	Ceiling Near SE Corner
21075	Shop Area	2.7	Dust Collector - North Side
20982	Room 13	1.9	South End
21062	Gym	1.8	Red Panels - SE
21065	Gym	1.8	Red Panels - NW
20996	Auditorium	1.6	Upper Stage
21054	Library	1.5	---
21078	Room 21	1.5	North End
20912	Home Economics	1.3	East End
21013	Home Economics	1.0	West End
21069	Shop Area	0.8	South Wall, SE End
21059	Boiler Room	0.7	Near Pumps, Duplicate With 21058
21058	Boiler Room	0.2	Near Pumps, Duplicate With 21059
20909	Auditorium	---	Detector Missing
21070	Multi-Purpose Room	---	Detector Missing

***Table A-3** (continued)*

Ashman Elementary School			
21074	First Grade	0.4	New Building; Middle of Room
20989	Tunnel	0.2	New Building
21071	Office	0.2	New Building; Above Cabinet
21060	Boiler Room	0.1	Old Building; Downstairs Tunnel
20900	Boiler Room	0.0	Old Building; Downstairs
20901	Entrance	0.0	Old Building; Front Entrance
20902	Third Grade	0.0	Old Building; Middle of Room
20903	Second Grade	0.0	Old Building; Middle of Room
20904	Boiler Room	0.0	Old Building; South Side
20906	Kitchen	0.0	Old Building; Office Area
20907	Multi-Purpose Room	0.0	Old Building; SW Corner
20908	Room 25	0.0	Old Building; North End
20913	Media Room	0.0	Old Building; Middle of Room
20980	Kindergarten	0.0	Old Building; West Side
20987	Room 19	0.0	Old Building; East End
20998	Pod	0.0	Old Building
21076	Pod Tunnel	0.0	Old Building; Left of Entrance
21080	Custodian Room	0.0	Old Building; Above Door